REPUBLIC OF TURKEY

YILDIZ TECHNICAL UNIVERSITY

GRADUATE SCHOOL OF SCIENCE AND ENGINEERING

PERFORMANCE ENHANCEMENT OF TURBOCHARGER CENTRIFUGAL COMPRESSOR

Mesut GUNEES

MASTER OF SCIENCE THESIS

Department of Mechanical Engineering

Energy Program

Supervisor

Assoc. Prof. Nader JAVANI

January, 2022

REPUBLIC OF TURKEY

YILDIZ TECHNICAL UNIVERSITY

GRADUATE SCHOOL OF SCIENCE AND ENGINEERING

PERFORMANCE ENHANCEMENT OF TURBOCHARGER CENTRIFUGAL COMPRESSOR

A thesis submitted by Mesut GUNEES in partial fulfillment of the requirements for the degree of MASTER'S THESIS is approved by the committee on 23.12.2021 in Department of Mechanical Engineering, Energy Program.

Assoc. Prof. Nader JAVANI
Yıldız Technical University
Supervisor

Approved By the Examining Committee

Assoc. Prof. Nader JAVANI, Supervisor
Yildiz Technical University ______________________________

Prof. Dr. Ali Volkan AKKAYA, Member
Yildiz Technical University ______________________________

Assis. Prof. Dr. Senem Şentürk Lüle, Member
Istanbul Technical University ______________________________

I hereby declare that I have obtained the required legal permissions during data collection and exploitation procedures, that I have made the in-text citations and cited the references properly, that I haven't falsified and/or fabricated research data and results of the study and that I have abided by the principles of the scientific research and ethics during my Thesis Study under the title of Performance Enhancement of Turbocharger Centrifugal Compressor supervised by my supervisor, Asst. Prof. Nader JAVANI. In the case of a discovery of false statement, I am to acknowledge any legal consequence.

Mesut GUNEES

Signature

Dedicated to my wife, my family,

and my friends

ACKNOWLEDGEMENTS

It would not be possible to complete this work without the countless help and support from many people around me, and it is only possible to give particular thanks to some of them here.

My esteemed supervisor, who did not withhold any kind of support from me during this study, and who constantly added new perspectives at different stages the studies, as well as his theoretical support, to Assoc. Prof. Nader JAVANI my sincere thanks.

I would like to express my respect and love to my dear family, the GUNEES and the KIR family who have always been by my side for their sincere help in every matter, thank you. I particularly wish to thank my dear wife, Gamze KIR GUNEES, who became an official member of our family in 2021, for her help, and embrace her with love and respect.

Since gratitude to BMC Power 1D CFD & Turbocharger Development Team Leader Ayberk PEKER, my colleagues Enes SAHIN, Fatih TEVKUR and Eda BILGIN, who made valuable contributions to the studies with technical knowledge and experience they provided throughout this process.

Thank you Emre AKI and Samet YALDIZ, you proved to be not only respectful housemates but also a real valuable person in every way.

Finally, I would also like to thank all the people and institutions who contributed to the completion of this study, my friends, and colleagues.

It should be noted that changes have been made to much of the detailed data to protect proprietary information.

Mesut GUNEES

TABLE OF CONTENTS

LIST OF SYMBOLS

C	Absolute flow velocity (m/s)
v	Absolute velocity (m/s)
a	Acceleration (m/s^2)
B	Aerodynamic blockage ()
A	Area (m2)
U	Blade speed (m/s)
_H	Compressor work input per unit mass (J/kg)
ρ	Density (kg/m3)
D	Diameter (m)
E	Energy (J)
F	Force (N)
R	Gas constant (J/kgK)
G	Gravitational acceleration (m/s^2)
Q	Heat (J)
u	Internal Energy (J)
η	Isentropic total to total efficiency ()
M_{a}	Mach number ()
$\dot{m}$	Mass flow rate (kg/s)
z	Number of blade ()
b	Passage height (m)
δ	Partial derivative
P	Power (W)
p	Pressure (Pa)
r	Radius (m)
w	Relative velocity (m/s)
σ	Slip factor
C_p	Specific heat capacity, constant pressure (J/kg K)
C_{v}	Specific heat capacity, constant volume (J/kg K)
θ	Tangential velocity component
τ	Torque (Nm)
T_0	Total temperature (K)

β_2 Trailing edge blade backsweep angle (considered positive if in impeller rotation direction) measured from radial (°)

W Work (J)

ψ Work input coefficient

LIST OF ABBREVIATIONS

u	Circumferential / tangential direction
CFD	Computational Fluid Dynamic
EGR	Exhaust gas recirculation
FGT	Fixed geometry turbine
g	Gauge
h	Hub
IGV	Inlet guide vanes
max	Maximum value for given parameter
PR	Pressure ratio
RMS	Root mean square
r	Radial direction
s	Shroud
SCR	Selective catalytic reduction
SST	Shear stress turbulence
th	Throat
VGT	Variable geometry turbine
WG	Wastegate

LIST OF FIGURES

LIST OF TABLES

ABSTRACT

Performance Enhancement of Turbocharger Centrifugal Compressor

Mesut GUNEES

Department of Mechanical Engineering

Master of Science Thesis

Supervisor: Assoc. Prof. Nader JAVANI

In this thesis, the compressor part of a turbocharger system is examined. In the turbocharger compressor performance map provided by the supplier, the efficiencies are not at the desired levels. For this reason, it has been tried to increase the efficiency of the operating points selected on the compressor map under the same conditions. The first step of the study is to analyze the compressor side geometries (compressor wheel, diffuser and volute). In order to perform the analysis, three different operating points (OP1-OP2-OP3) are selected from the critical regions of the performance map. The numerical analysis of the existing compressor is performed at these three points. It is seen that the efficiency error rates between the analysis and the experiment data are %1.6 (OP1), %0.9 (OP2) and %3.1 (OP3). This proves that our CFD model is validated based on the experimental data. The second part of the study is started with an examination of the impeller. Literature studies on increasing the performance of the compressor system are examined in detail. As a result of the literature research, it has been seen that the centrifugal compressor backsweep angle at the outlet of the blade (β2) and total blade number of blades (z) design parameters have significant effects on turbocharger compressor performance. A total of 45 different CFD models are defined for a total of 15 different designs (including the original design) at three different operating points and analyzed on the validated CFD model in order the examine the effect of the blade backsweep angle (β2) at compressor wheel outlet and total blade number combination on performance. For the total number of blades, a total of twelve (six – six (main blades– splitter blades)), a total of fourteen (seven – seven) and a total of sixteen (eight – eight) (original compressor wheel) are examined. In addition, 5 different trailing edge backsweep angles (20°, 22.5°, 25°, 27.5° (original angle of compressor wheel), and 30°) are considered.

Within the scope of this thesis, efficiency gains at levels where pressure variation is negligible are taken into account. Efficiency and pressure variations of all designs, including the current impeller design, are evaluated on the same graphs for the same operating points, and the blade backsweep angle is reduced 2.5°, while the total number of blades is reduced from 16 to 14. The results of the analyzes performed with the existing impeller design are compared in terms of compressor outlet pressure and compressor isentropic efficiency. At the first operating point, an increase of 0.78% is achieved in the isentropic efficiency of the compressor when the total outlet pressure variation is 0.58%. In the case where the total outlet pressure change at the second operating point was 0.68% an efficiency increase of 1.98% is achieved. Finally, when the third operating point is examined, a 2.34% improvement in the isentropic efficiency of the compressor is obtained when the total pressure change at the compressor outlet is 0.35%. The greatest efficiency increase is seen in OP2 and the greatest pressure change is observed in OP3.

Keywords: Turbocharger, Centrifugal compressor, Blade backsweep angle, Total number of blades, Performance

---

YILDIZ TECHNICAL UNIVERSITY

GRADUATE SCHOOL OF SCIENCE AND ENGINEERING

ÖZET

Turboşarj Santrifüj Kompresörünün Performans İyileştirmesi

Mesut GUNEES

Makine Mühendisliği Bölümü

Yüksek Lisans Tezi

Danışman: Doç. Dr. Nader JAVANI

Bu tez çalışmasında, turboşarj sisteminin kompresör bölümü incelenmiştir. Tedarikçi tarafından sağlanan turboşarj kompresör performans haritasında verimlerin istenilen seviyelerde olmadığı görülmüştür. Bu nedenle, kompresör haritasının kritik görülen bölgelerinden 3 farklı çalışma noktası (ÇN1- ÇN2- ÇN3) seçilmiştir, seçilen noktalarda aynı koşullarda verimlilikler arttırılmaya çalışılmıştır. Çalışmanın ilk adımını kompresör sistemi geometrilerinin (kompresör çarkı, difüzör ve volüt (salyangoz)) analiz edilmesi oluşturmaktadır. Mevcut kompresörün sayısal analizi bu üç noktada gerçekleştirilmiştir. Analiz ve test verileri arasındaki verimlilik hata oranlarının %1,6 (ÇN1), %0,9 (ÇN2) and %3,1 (ÇN3) olduğu görülmüştür. Bu da CFD modelimizin deney datalarına binaen valide edildiğini göstermektedir. Kompresör geometrisinin sayısal analizlerle doğrulanmasının ardından çalışmanın ikinci kısmında çark üzerinde incelemeye geçilmiştir. Kompresör sistemi performansının arttırılması üzerine yapılan literatür çalışmaları detaylı bir şekilde incelenmiştir. Yapılan literatür araştırması sonucu, kanat çıkışındaki santrifüj kompresör geri süpürme açısı (β2) ve toplam kanat sayısı parametrelerinin performans üzerinde önemli etkilerinin olduğu görülmüştür. Kompresör çark çıkışındaki kanat geri süpürme açısının (β2) ve toplam kanat sayısı

kombinasyonunun performansa etkisini irdelemek için toplam 15 farklı tasarım (orijinal tasarım dahil) ve üç farklı nokta çalışma noktası için toplam 45 farklı CFD modeli oluşturulmuştur ve valide edilmiş CFD modeli üzerinde analiz edilmiştir. Toplam kanat sayısı için toplam on iki (altı – altı (ana kanatlar – ayırıcı kanatlar)), toplam on dört (yedi – yedi) ve toplam on altı (sekiz – sekiz) (orijinale kompresör çarkı) incelenmiştir. Ayrıca, 5 farklı kanat çıkış geri süpürme açısı (20°, 22,5°, 25°, 27,5° (kompresör çarkının orijinal açısı), ve 30°) oluşturulmuştur.

Bu tez çalışması kapsamında, basınç değişiminin göz ardı edilebilir olduğu seviyelerdeki verimlilik artışı dikkate alınmıştır. Mevcut çark tasarımı dahil olmak üzere tüm tasarımların verimlilik ve basınç değişimleri aynı çalışma noktası için aynı grafikler üzerinde değerlendirilmiştir ve kanat geri süpürme açısı 2,5° azaltılırken, toplam kanat sayısı da 16'dan 14'e düşürülmüştür. Mevcut çark tasarımı ve yeni çark tasarımı ile gerçekleştirilen analizlerin sonuçları kompresör çıkış toplam basıncı ve kompresör izentropik verimi bakımından karşılaştırılmıştır. Birinci çalışma noktasında, çıkış toplam basıncı değişiminin %0,58 olduğu durumda kompresörün izentropik verimliliğinde %0,78'lik bir artış sağlanmıştır. İkinci çalışma noktasında toplam çıkış basıncı değişiminin %0,68 olduğu durumda %1,98'lik verim artışına ulaşılmıştır. Son olarak da üçüncü çalışma noktası incelendiğinde kompresör çıkışı toplam basıncı değişiminin %0,35 olduğu durumda kompresörün izentropik verimliliğinde %2,34'lük bir iyileşme elde edilmiştir. En büyük verim artışı OP2'de ve en büyük basınç değişimi OP3'te görülmüştür.

Anahtar Kelimeler: Turboşarj, santrifüj kompresör, kanat çıkış açısı, toplam kanat sayısı, performans.

1
INTRODUCTION

1.1 Literature Review

There are many studies on the compressor in the literature. Most of them are about improvement the compressor's surge and choke limits. However, there are also studies to increase compressor efficiency. Among these studies, studies examining the impeller design, which is the heart of the compressor, are predominant. In this section, literature studies on the effects of impeller design on compressor efficiency are given. By examining these studies, the list that affects the design of the wheel in Section 4 is the list.

Rodgers and Sapiro developed one-dimensional models for the conditions that cause pressure loss and efficiency reduction, such as blade tip flow and friction, to obtain the optimum compressor design in term of aerodynamics. With the developed models, the effects of blade outlet angle between 0° - 30° and prewhirl between 0° - 40° in compressors with pressure ratios between 3 and 9 were investigated. As a result of the study, they determined that the use of pre-rotation had a positive effect on the efficiency of the compressor. In addition, the blade outlet angle being greater than 0° (i.e., the blades are not radial) increases the efficiency. Rodgers and Sapiro stated that the main reason for the efficiency increase obtained with this blade outlet angle and pre-rotation is the decrease in the relative Mach numbers at the impeller inlet and the absolute Mach numbers at the impeller outlet. In addition, designs such as double inlet impeller, tandem impeller inlet, rotating diffuser, semi-axial impeller (mixed flow) and splitter blade are also included in the study to increase the efficiency of compressor with the high-pressure ratio (>5), where high Mach number causes flow losses [1].

Rodgers, in his study, examined the effect of the number of blades on the efficiency of the centrifugal compressor wheel and aimed to find the optimum number of blades. He validated the one-dimensional model that he created for friction losses during efficiency calculations with experimental data. One of the most important outputs of the study is that the optimum number of blades varies according to the specific speed of compressor. Rodgers showed at the end of his work that the optimum number of blades can be expressed as a function of the blade's exit angle and the specific speed of the impeller [2].

Hilderbrant and Genrup numerically investigated the effect of blade outlet angle (backsweep) and blade outlet width on outlet flow in a centrifugal compressor with a vaneless diffuser. Two different blade backsweep angles (45° and 38°) and three different exducer widths (original, original*0.925 and original*1.075) were considered in the studies. Hilderbrant and Genrup, who supported the one-dimensional models they created with three-dimensional analysis, achieved the highest efficiency of the compressor with the original blade exducer width. However, as a result of the study, it was observed that the increased blade outlet backsweep angle provides a more homogeneous velocity distribution at the impeller outlet [3].

Saravanamuttoo, Cohen and Rogers mentioned that an increase in the number of blades will increase the slip factor, which will increase the solidity of impeller eye and decrease in the effective flow area. This will increase the velocity at the inlet to compensate for the loss of flow area [4].

The relationship is showed by Busemann and Lewis for the variation of the slip factor according to the number of blades of the impeller and the inlet-outlet diameter ratio. They proved that losses will increase when number of blades are increased [5]. In addition, increasing the number of blades will increase the weight of the impeller and may lead to an update in the bearing system.

Seiichi and Isao, in their study, changed design parameters and created 2 different design options according to the existing wheel. One of the updated impeller design parameters they updated is the total number of blades. By reducing the total number of blades on the existed wheel from 6+6 to 5+5, an increase in efficiency was successfully achieved in one of the design options [6]. More friction loss will occur in the impeller with more blades than two impellers with the same mass flow rate. The first reason for this is the decrease in the area that the flow can pass at the impeller inlet with the increasing number of blades, the increase in the flow velocity and the increase in the Reynolds number. The second reason is that the friction surface increases with the increase in the number of blades.

Tie Wang and Cheng Peng created 8 different designs by changing blade back sweep angle as 0°, 2.5°, 5°, 7.5°, 10°, 12.5°, 15°, 17.5°. They examined the results regarding engine speed which is between 500 – 4500 RPM. They stated that shock waves occurred on splitter blade root when the backsweep angle is increased. As the back sweep angle increases, the scope of shock wave expands. The shock wave significantly reduces the velocity at the blade outlet. The shock wave can cause a loss of total pressure. In addition, increasing back sweep angle provides an increase in isentropic efficiency in the 1000 RPM to 2000 RPM range [7].

1.2 Objective of the Thesis

A well-performing turbocharger is an essential part of achieving lower fuel consumption and CO2 emissions in an internal combustion engine.

It has been observed that the compressor efficiency is lower than the desired level in the turbocharger system supplied from the its manufacturer. The low compressor efficiency negatively affects the fuel consumption and emission values of entire system. A new design and development tool was acquired therefore, with the help of these new tools, it may be possible to improve the performance of the unit by updating the compressor design, thus achieving lower fuel consumption and lower CO2 emissions. In this thesis, the effects of the design parameters of the impeller, which is the most important part of the compressor, on the compressor efficiency were examined, and it was aimed to increase the efficiency of the existing compressor with the new impeller design.

1.3 Hypothesis

In this thesis, studies will be carried out to improve the isentropic efficiecny of the centrifugal compressor of the turbocharger system. At the beginning of this study, three operating points will be selected on the experimental compressor map. These operating points are selected from the critical regions of the compressor map that the internal combustion engine manufacturer takes into account during the turbocharger selection phase. As the first step of the study, the CFD model of the compressor, whose 3D model is obtained, will be created and analyzed at the selected operating points and model data will be verified according to the test data. As the second step of the study, it is aimed to increase compressor isentropic efficiency at the selected 3 operating points by changing the compressor total number of blades and blade outlet backsweep angle parameters using the verified CFD model.

1.4 History and Development

The word turbocharger or turbo is derived from the Greek word "τύρβη" which means "mixing/rotating". In internal combustion engines, it is a tool that helps to obtain higher power from the same engine volume by pressing more air into the combustion chamber. While doing this, two different systems are used as the working principle; the first is the turbocharger and the second is the supercharger. The main difference in the operating principles is the mechanism that is driven. In turbochargers, the compressor part is driven by the turbine, which is converted by the energy of the exhaust gas coming out of the engine's exhaust manifold and the compressor part in superchargers takes the energy from the flywheel of the engine. The turbocharged engine schematic view is shown in Figure 1.1 and supercharged engine schematic view is shown in Figure 1.2.

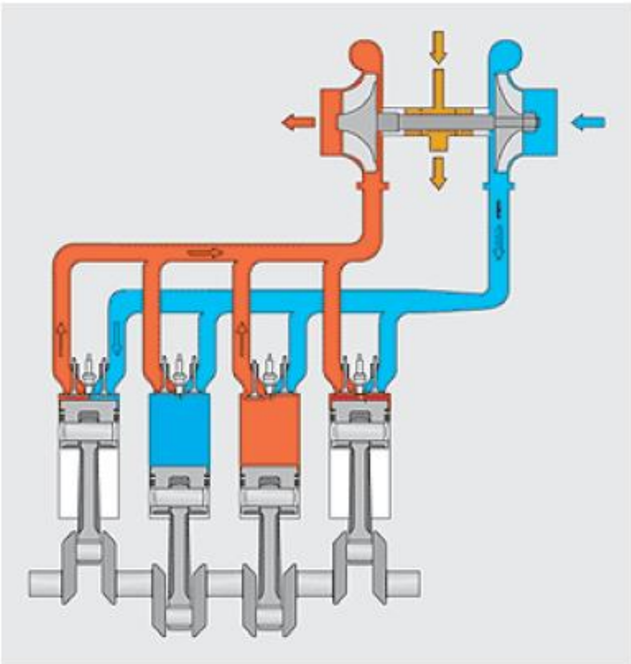

Figure 1. 1 Turbocharger schematic view [8]

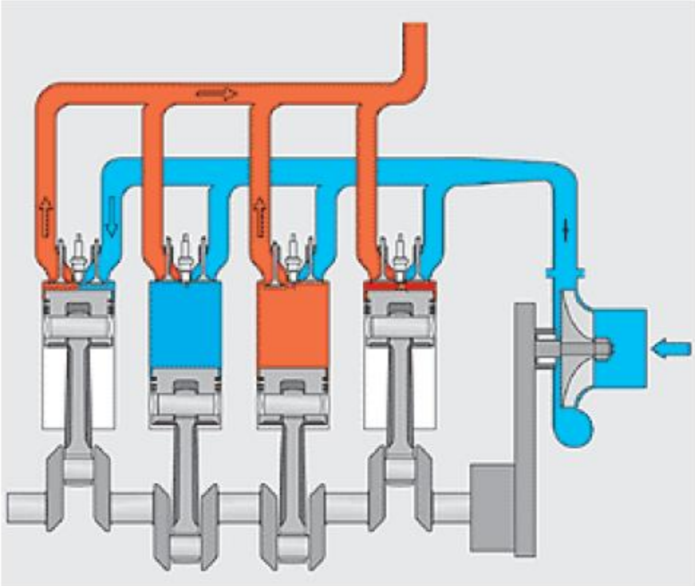

Figure 1. 2 Supercharger schematic view [8]

The history of turbocharging is as old as the history of internal combustion engines. At the end of the 19th century, the efforts of Gottlieb Daimler and Rudolf Diesel to reduce fuel consumption, as well as to increase the power they got from the engine were based on the principle of pushing the combustion gases back into the engine. Alfred Buchi was the first to successfully invent the generation of energy from exhaust gases in 1925. Buchi was providing a 40% increase in power with the newly developed system. This application was the first use of the turbocharger in the automotive industry. In the following years, this system started to be used mostly in sea vehicles with large engines. In 1938, it was used for the first time by a Swedish truck manufacturer. The first cars with turbochargers were introduced in the United States in 1962 by the Chevrolet Company on gasoline vehicles. The first diesel vehicle was used by Mercedes-Benz in 1978. When we look at today, almost all diesel vehicles use a turbocharger. In gasoline vehicles, on the other hand, it continues to be used to save fuel rather than increase power as in previous times [8-9].

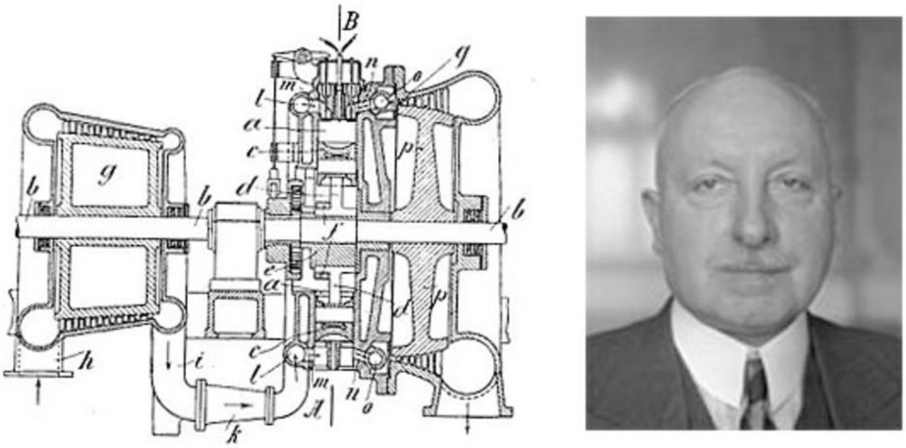

Figure 1. 3 Alfred Buchi portrait and his turbocharger system patent scheme [10]

1.5 Internal Combustion Engines

An internal combustion engine is a vehicle in which the energies of high temperature and high-pressure gasses, which are formed because of the combustion reaction with the oxidation of fuels, are converted into motion energy by applying them to mechanical part. Fossil fuels are generally used as fuel. For oxidation, fresh air is the ideal tool. Usable mechanical energy is obtained by passing the products of high pressure and high temperature combustion reaction through a piston-cylinder-crank mechanism. The engine developed by Samuel Morey, who first patented the internal combustion engine, can be observed in the image below.

Figure 1. 4 Internal combustion engine developed by Samuel Moray [11]

Internal combustion engines are widely used in transportation vehicles such as automobiles, airplanes, helicopters, ships. In addition, internal combustion engines are used in applications such as electric generators and fluid pumping. Internal combustion engines can be classified according to many different characteristics. However, within the scope of thesis, internal combustion engines can be grouped into two main groups. The first of these group is 2-stroke and 4-stroke piston engines and various types of these engines and rotary engines such as Wankel. 4-stroke schematic is shown in Figure 1.5.

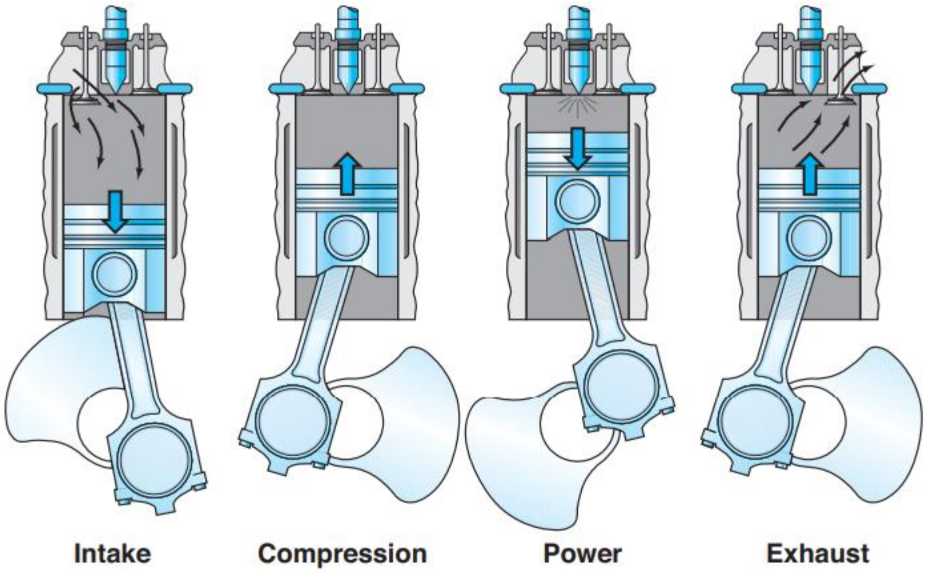

Figure 1. 5 The four-stroke cycle [12]

The second group includes gas turbines, jet engines and rocket engines. The specific power of the second group of engines is quite high and the combustion continues continuously. The engines in the first group are the engines that are the subject of the thesis. Undoubtedly, the engines used in today's automotive industry and customized for land vehicles are 4-stroke engines.

1.5.1 Thermodynamic Cycles in Engines

4-stroke engines can operate according to different thermodynamic cycles. With this cycle, Otto (constant volume heat input cycle), Diesel (constant pressure heat input cycle) and mixed cycles are derived from these two cycles. The Otto cycle is the ideal cycle of today's gasoline engines within a set of thermodynamic assumptions and the P-V diagram and T-s diagram of the cycle are shown below.

1-2 ↔ Adiabatic compression

2-3 ↔ Constant heat input

3-4 ↔ Adiabatic expansion

4-1 ↔ Constant volume heat output

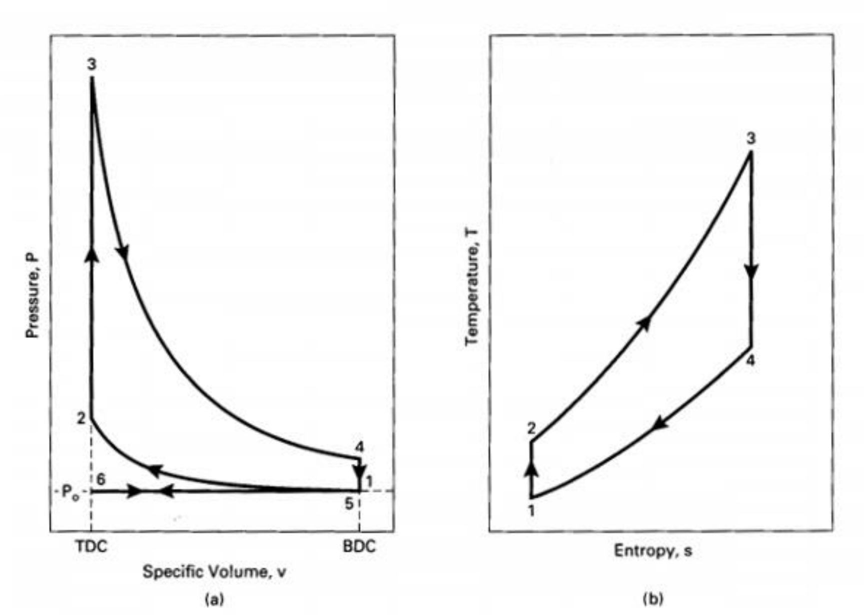

Figure 1. 6 Otto cycle, 6-1-2-3-4-5-6, On (a) pressure-specific volume coordinates, and (b) temperature-entropy coordinates [12]

Diesel cycle consists of the following steps and P-V, T-s diagrams are shown in Figure 1.7.

1-2 ↔ Adiabatic compression

2-3 ↔ Constant pressure heat output

3-4 ↔ Adiabatic expansion

4-1 ↔ Constant volume heat output

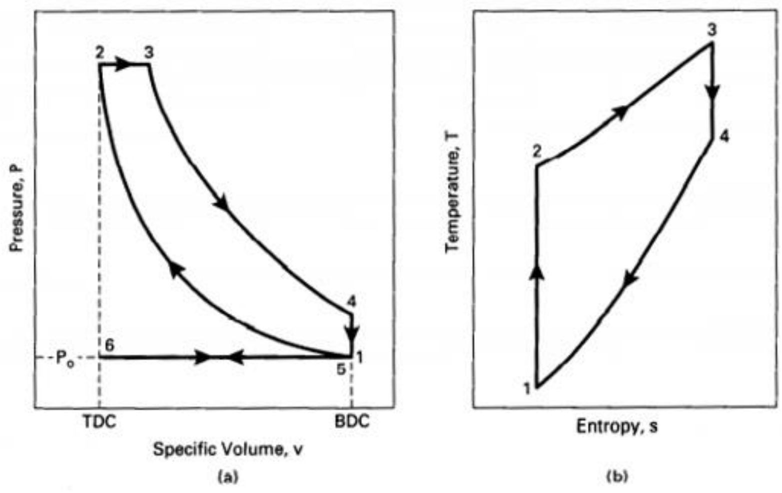

Figure 1. 7 Diesel cycle, 6-1-2-3-4-5-6 (a) pressure-specific volume coordinates and (b) temperature-entropy coordinates [12]

The dual cycle (seilinger) can be defined as a combined and modified version of the Otto and the Diesel cycles.

The dual cycle consists of the following steps and P-V, T-s diagrams are shown in Figure 1.8.

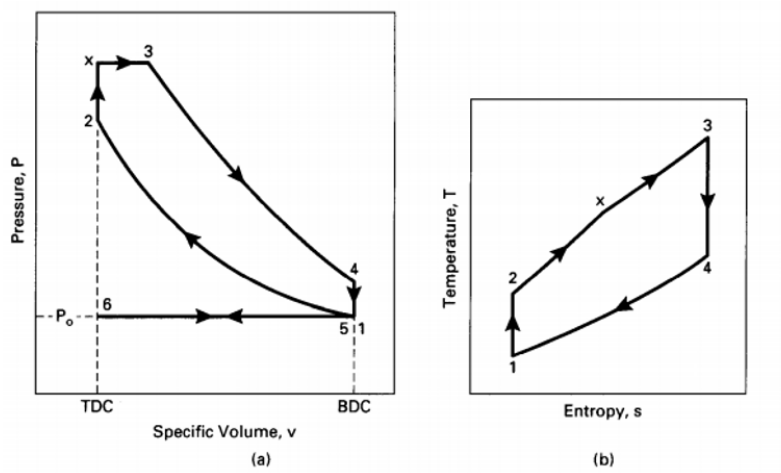

Figure 1. 8 Dual cycle, 6-1-2-x-3-4-5-6 (a) pressure-specific volume coordinates, and (b) temperature-entropy coordinates [12]

1-2 ↔ Adiabatic compression

2-3 ↔ Constant heat output

3-4 ↔ Constant pressure heat output

4-1 ↔ Adiabatic expansion

5-1 ↔ Constant volume heat output

Below, the operating curves of the cycles are shown on the same graph for a more accurate comparison of these three cycles.

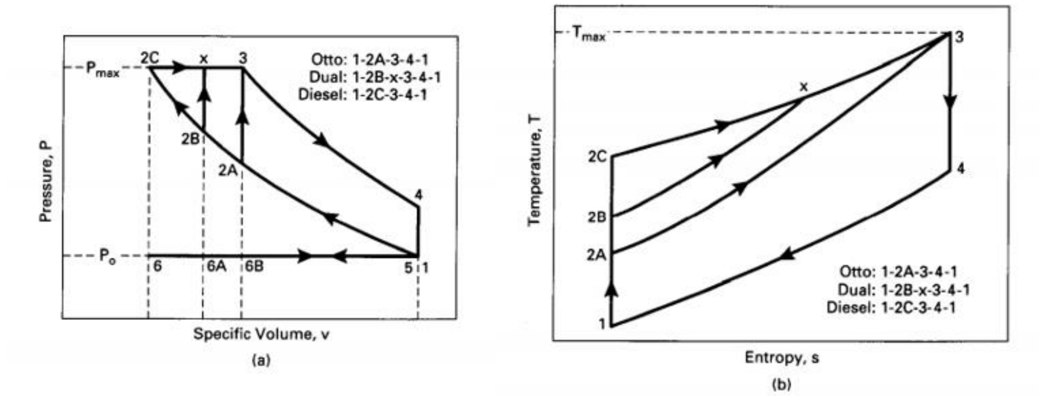

Figure 1. 9 Comparison of otto cycle, dual cycle, and diesel cycle. All engines have the same cylinder input conditions and the same maximum temperature and pressure (a) pressure-specific volume coordinates, and (b) temperature-entropy coordinates [12]

At the same compression ratio, the Otto cycle is the most efficient. The lowest efficient cycle is the Diesel cycle among these 3 cycles. However, Otto cycle engines have a lower compression ratio (8-11) due to the danger of knocking combustion. Diesel cycle engines have a higher compression ratio (16-18), so their efficiency is higher, and their fuel consumption is lower.

1.5.2 Reciprocating Internal Combustion Engines

Reciprocating engines used in automotive applications generally operate as four-stroke. A complete cycle during this combustion consists of 4 different times: Intake, Compression, Power (expansion and combustion), and Exhaust. The operating times of the four-stroke engine according to the above-mentioned cycles are as follows:

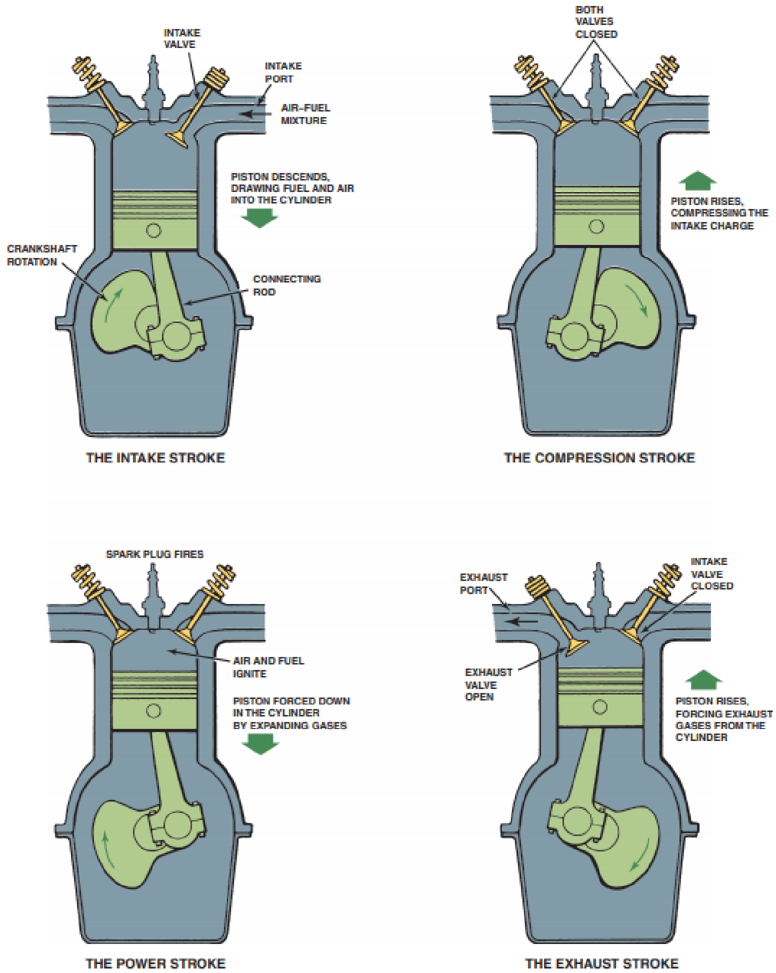

Figure 1. 10 Cycles of four-stroke engines [13]

<u>Intake Stroke:</u> At this time, the fuel-air mixture is sent into the cylinder. At the beginning of this time, the piston is in what is known as the Top Dead Center. So, there is minimal clearance in the cylinder at the top of the piston. As the piston descends, the intake valves open and the fuel-air mixture fills the cylinder. Intake stroke indicates the time when the fuel-air mixture is sent into the cylinder where combustion will take place and is the beginning of the cycle of four-stroke internal combustion engines.

<u>Compression Stroke:</u> When the piston reaches the lowest point, which is called the bottom dead point, the suction ends. The piston starts moving upwards again. At this time, the intake valves are closed, and the volume of the intake fuel-air mixture begins to decrease. As the volume decreases, pressure and temperature rise. The volume in the cylinder is reduced approximately 8-12 time in gasoline engines and 16-18 time is diesel engines during compression time.

Power (Expansion and Combustion) Stroke: In gasoline engines, when the cylinder reaches the top dead center (when there is maximum compression), the mixture is ignited by ignition with spark plugs. Combustion develops very quickly and the pressure that rises suddenly due to the released energy forces the piston to descend. As the gases expand, they spend most of the energy generated by combustion to push the piston down, and vehicle moves in this way. In diesel engines, the fuel-air mixture ignites spontaneously due to the temperature rise just before the piston reaches top dead center. Combustion is slower that gasoline engines and continues for a certain part of the power stroke.

Exhaust Stroke: The piston, which reaches the bottom dead center because of expansion, moves upwards again. At this time, the exhaust valves are opened, and the burned gases are thrown out. At the end of this time, some exhaust gas will remain in the upper dead volume. Then, while the exhaust valves are closed, the intake valves open and the engine starts the intake stroke again.

In this thesis, turbocharger system is developed for an engine that operates four-stroke cycle.

1.6 Principles of Turbocharging

1.6.1 Power Augmentation

The power from an internal combustion engine is defined by the formula: -

$$P = P_m \; x \; d^2 x \; s \; x \; n \; x \; N \qquad (1.1)$$

In this formula, P is engine power, Pm is brake mean effective pressure, d is cylinder bore, s is engine stroke, n is the number of cylinders and N is engine speed.

As a result of increasing any of these parameters, the power taken from the engine will also increase. However, cylinder bore, engine stroke, number of cylinders and engine speed are parameters that cannot be changed due to the mechanical design of the engine. However, the BMEP value is not completely unchangeable.

Brake mean effective pressure (BMEP) is the average pressure of the entire cycle reduced to stroke volume. This value increases with the increase of combustion pressure. Although high in-cylinder pressure and temperatures cause the pistons and cylinders to be subjected to more mechanical thermal stress and more NOx emission with increasing temperature, it is most feasible to increase to BMEP value instead of other parameters.

To increase BMEP, it is basically necessary to increase the reaction that place takes place in the combustion chamber. More simply, increasing the fuel delivered into the cylinder means reaching higher BMEP values. But for more fuel to be burned, more fresh air will also need to be sent into the cylinder. Otherwise, the low air content will be a constraint for the combustion reaction and the necessary energy will not be released to reach high BMEP values. Sending more air into the cylinder can be called turbocharging [14].

Turbocharger system ensures that fresh air with higher density and pressure is pushed into the cylinder.

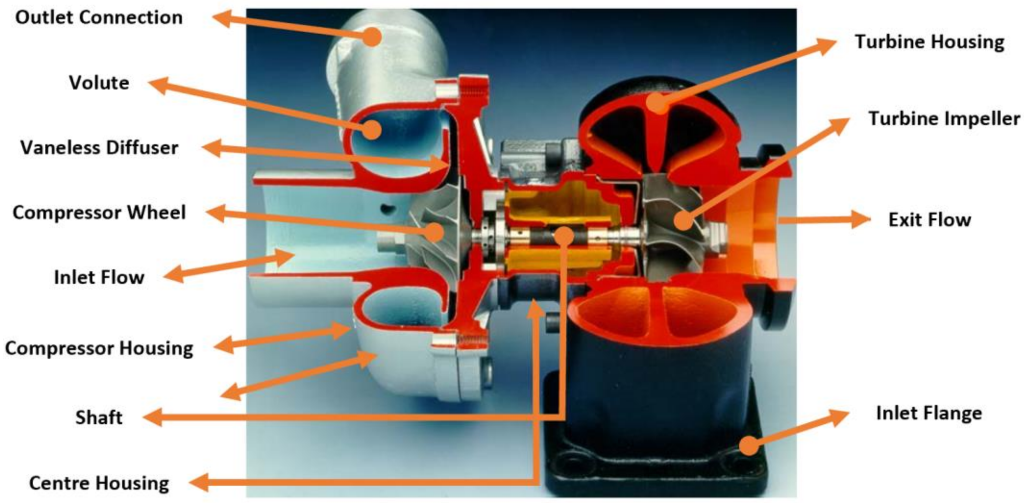

Figure 1. 11 Turbocharger system sections

1.6.2 Advantages of Turbocharging

The turbocharger system performs supercharging with the help of a compressor wheel. Fresh air is sent to the combustion chamber under pressure by driving the compressor wheel with an external force. The external force that drives the compressor wheel is the turbine wheel mounted on the compressor wheel with a common shaft. Turbine wheels can have different geometries as radial, axial and mixed. However, turbines in the automotive sector are mostly turbines with radial geometry. Below is the Figure 1.12 showing the geometries of the different turbines.

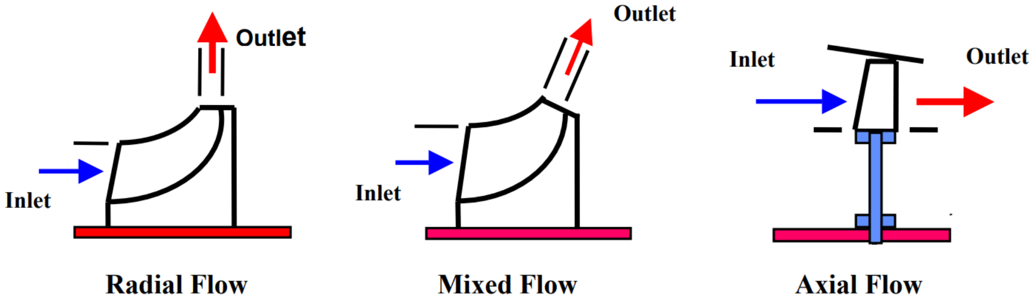

Figure 1. 12 Radial, mixed and axial flow turbine [14]

The turbine uses the enthalpy of high pressure and temperature exhaust gases after the explosion in the combustion chamber and is located on the exhaust side of the internal combustion engine (usually mounted on the engine just after the exhaust manifold). Due to the temperature and pressure of the exhaust gasses formed as a result of the combustion reaction in the combustion chamber, its enthalpy is converted into motion in the turbine wheel. This motion energy is transmitted to the compressor wheel via a common shaft mentioned above, and the clean air with atmospheric pressure is pressurized and sent to the combustion chamber. Thus, the engine now becomes a supercharged engine instead of a naturally aspirated engine. These gas flow processes can be observed in the diagram below. In addition to the ones mentioned above, there is also an intercooler in the diagram. The task of this cooler is to reduce the increasing temperature of the fresh air pressurized in the compressor before it enters the combustion chamber and to increase its density. Thus, the air mass entering the combustion chamber will be increased.

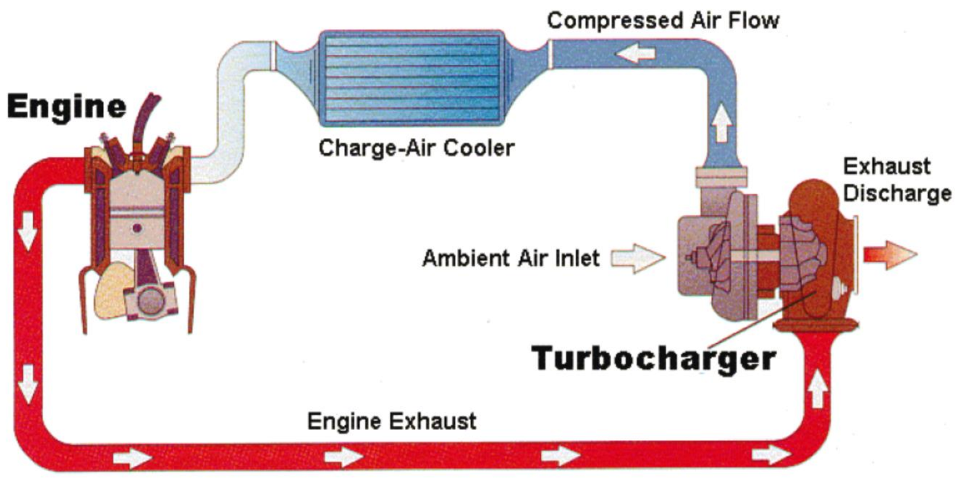

Figure 1. 13 Turbocharging system and engine airflow diagram [15]

The turbocharger system enables the engine to transform a naturally aspirated system to a turbocharged system, thus increasing the performance of an engine. Therefore, the most important effect of the turbocharger system on the engine is its positive effect on performance and fuel consumption. When we compare an engine with a turbocharger system and naturally aspirated engine, we can see the following main differences:

Engine weight: There is a significant weight difference between a turbocharged engine with the same power and a naturally aspirated engine. In order to achieve the performance difference brought by the turbocharger system with a naturally aspirated engine, it is necessary to increase the volume of the naturally aspirated engine, thus increasing the engine weight. In summary, the turbocharger system increases the power density of the engine [16].

Fuel Consumption: With the decrease in engine volume, the energy going from the engine to the friction also decreases. In addition, the exhaust energy that wasted in naturally aspirated engines is passed through the turbine in turbocharged engines and its energy is used and returned to the system. This brings an additional engine efficiency increase. And, ensuring that the fresh air sent to the combustion chamber is higher in mass than naturally aspirated systems, maximizes the efficiency of combustion. This increase in combustion efficiency has a direct positive effect on fuel economy.

Exhaust Emission: The increased combustion efficiency leads to a decrease in the emission levels of the exhaust gases due to the fact that more power is obtained from smaller engines [16].

High Altitude Performance: Naturally aspirated engines are subject to performance loss due to the decrease in atmospheric pressure at high altitudes. This is not exactly true for engines with turbocharger systems. Because as the number of air decreases, the exhaust gas temperatures (energy) will increase, so the turbine power increases, and decreased air amount is increased again in this way [16].

Noise: The fact that turbocharged engines are smaller than naturally aspirated allows the engine to run less noisy. Sound sources in a small engine have lower levels than a larger engine. In addition, the turbocharged system also acts as a muffler in the exhaust path.

2
COMPRESSOR

In chapter 2, the basic background about dynamic compressor and the design details are described. You can find details of the geometry, definition of velocity triangles and flow through the blade passages are mentioned.

2.1 Classification of Compressor

Compressors are fluid dynamic-based machined that increase the pressure of the fluid by converting mechanical energy into potential energy. Compressors are divided into “dynamic” and “positive displacement”.

Positive displacement compressors increase the pressure of the fluid by reducing its volume. Since the flow rate of the fluid in this type of compressor depends on the volume swept per unit time, it changes linearly with the number of rotations.

Unlike positive displacement compressors, dynamic compressors perform the pressurization by accelerated and compressing the fluid. The flow, which is accelerated by the blades on the rotating wheel, is the slowed down by being inserted into a diffuser and the mechanical energy is converted into potential energy and pressure. All these systems, such as water turbines, gas turbines, pumps, and compressors, are also referred to as “turbomachines”. Dynamic compressors have many advantages over positive displacement compressors. The most important of these is that it is smaller than the pump of the same power, takes up less space and is light. Figure 2.1 shows the classification chart for dynamic and positive displacement compressors.

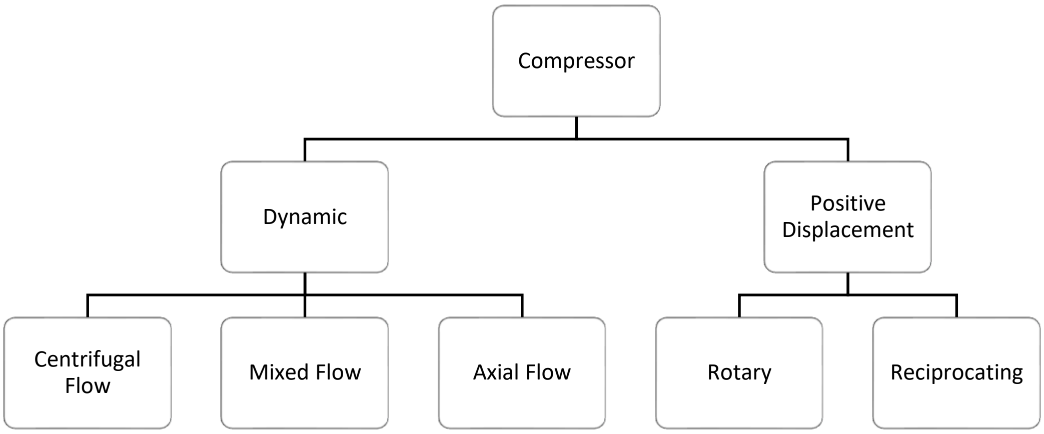

Figure 2. 1 Classification of compressor

Dynamic compressors are considered in three categories as radial centrifugal, side-channel (mixed flow) and axial. In axial compressors, the fluid moves parallel to the axis of rotation of the impeller, see figure 2.2. In axial compressor, which generally consist of more than one stage, the pressurization process takes place by the movement of the fluid through the passage consisting of high-speed rotating impeller blades and stationary blades. Centrifugal compressors are generally single stage. In centrifugal compressor, the fluid is accelerated by the blades on a high-speed rotating impeller, while the speed of the fluid coming to the diffuser after the impeller decreases, its pressure increases and passes through the diffuser and collects in the volute part.

Centrifugal compressors are widely preferred in turbochargers used in today's automotive engines, as they can reach higher pressure ratios and have a smaller volume compared to single-stage axial compressors. Axial compressor, on the other hand, are preferred in the aviation industry as they have a smaller front area that reduces aerodynamic resistance compared to centrifugal compressors and can perform the same pressurization with higher efficiency.

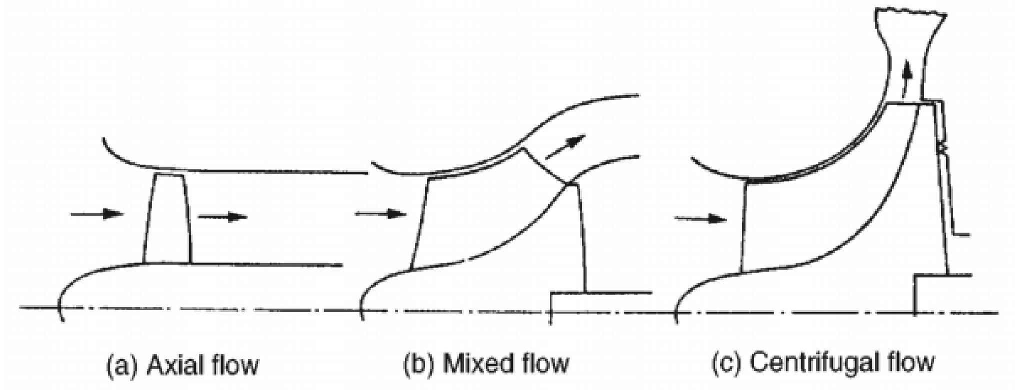

Figure 2. 2 Dynamic compressor types [17]

2.2 Centrifugal Compressor

Centrifugal compressors basically consist of five main parts: inlet, impeller, diffuser, volute and shroud (ported or not). The detailed diagram of the centrifugal compressor is shown in Figure 2.3 [18]. The so-called inlet is a channel whose purpose is to bring the incoming flow to the inducer stage of the impeller in a nearly uniform state. The flow entering the impeller at the inlet rotates by following blades and continues in the radial direction, reaching the output of the impeller (exducer) which is before the diffuser section. Thus, the flow is both rotated 90° and pressurized inside the impeller. The flow passes through the diffuser after leaving the impeller. The diffuser transmits the flow from the impeller to the volute. As the flow progresses through the diffuser, it slows down as the cross-sectional area increases, its kinetic energy decreases, and the static pressure increases. The air finally flows from the diffuser to the volute. The volute is the structure that transmits the flow from the diffuser to the outlet pipe. Generally, it has an increasing circular cross section towards the exit and is formed by rotating this section 360° around the diffuser. Similar to the diffuser, the kinetic energy of the flow is converted into pressure with increasing area in the volute, resulting in an increase in static pressure. In this thesis, the focus in on the impeller part of compressor.

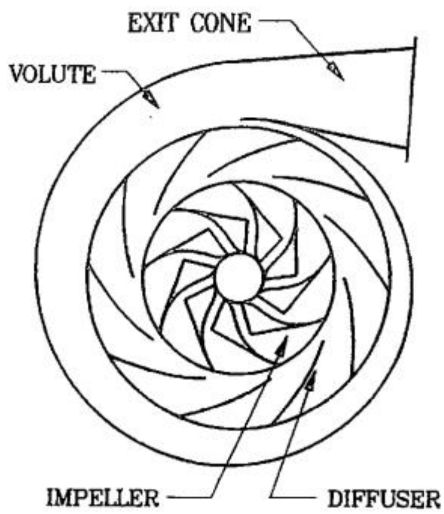

Figure 2. 3 Front view of a single stage compressor [18]

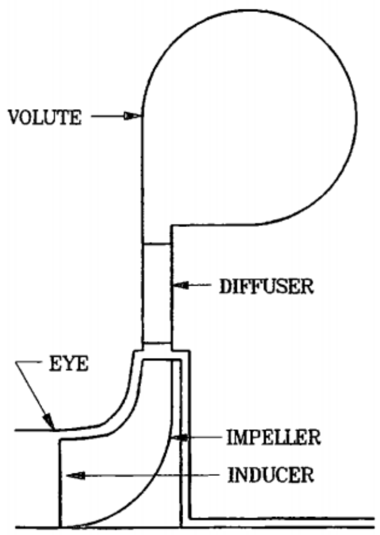

Figure 2. 4 Side view of a single stage compressor [18]

2.2.1 Compressor Inlet

The inlet of compressors ensures that air taken from the outside is carried to the compressor wheel. It is desirable to make the entrance part, which is generally in the form of circular pipe, as straight as possible in order to avoid local losses. However, due to the positioning of other elements in the engine and packaging problems, some parts of it may be curved. The inlet parts of the compressors can be in the form of straight pipes or vanes. These blades, called inlet guide vanes, are located just in front of the impeller and allow the inlet air to enter the impeller at a certain angle. In some of the compressors whose operating point is close to surge point, there are structures called "ported shroud", which provide aerodynamic stability and expand the operating range of the compressor by sending the recirculated fluid in the impeller back to the inlet. The ported shroud provides advantage in both surge and choke regions of compressor operation. Figure 2.5 shows the operation of ported shroud near the surge region.

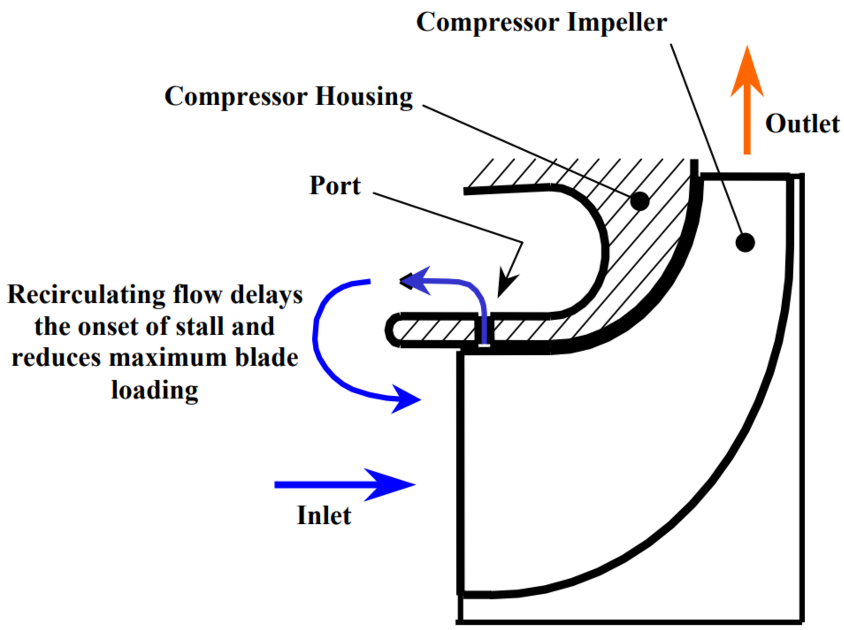

Figure 2. 5 Ported shroud operation near the surge region [2]

When the compressor is operated close to the choke region, the ported shroud also offers advantages. Figure 2.6 shows the effects of ported shroud treatment closer to choke flow.

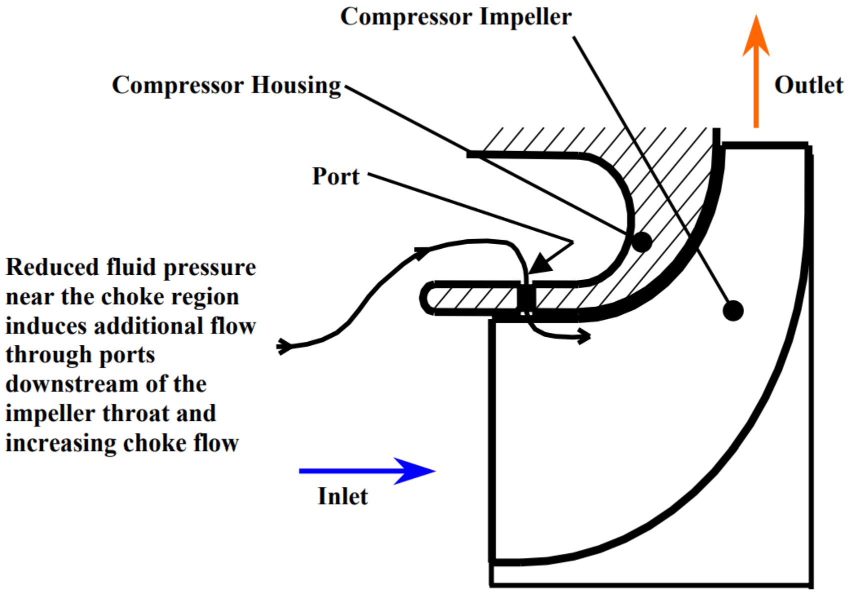

Figure 2. 6 Ported shroud operation near the choke region [2]

2.2.2 Compressor Impeller

In the radial flow compressor wheel, energy transfer occurs due to the rotation of the impeller, accompanied by an increase in the stagnation pressure and enthalpy of the fluid. Ensuring efficient diffusion of the working fluid both the impeller and diffuser is important for desired compressor stage efficiency.

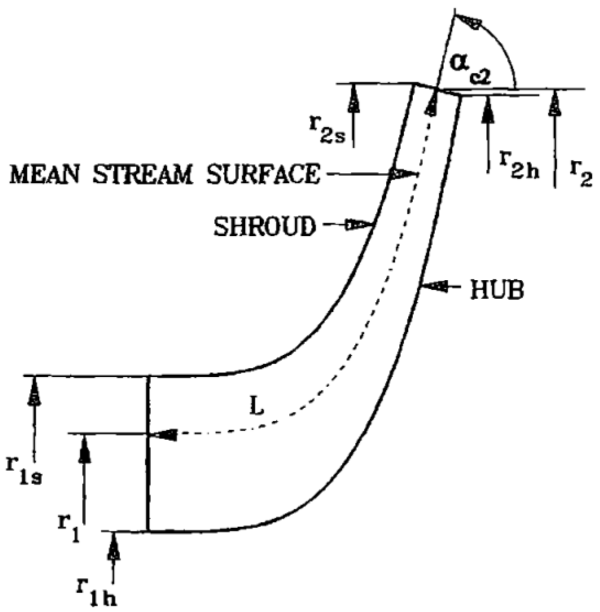

Figure 2. 7 Impeller passage geometry [18]

The only rotating aerodynamic element of the compressor stage is the impeller. All the kinetic energy given to the fluid is provided by the impeller and can provide a pressure increase of up to 70%, depending on design. In addition, the impeller is the basic element that allows the fluid working in the compressor to be taken in. Since the fluid must be drawn into the impeller at the beginning, the impeller provides the static pressure drop at the inlet. In this way, it ensures that fluid in front of impeller enters into the impeller and compressor.

If the blade starts at the impeller entrance and continues until the impeller exit, it is called a full blade. If the blade starts after a certain distance from the impeller entrance and ends at the impeller exit, it is called a splitter blade. While all the blades of the compressor impeller can be full blades, some of blades can also be composed of splitter blades, see in Figure 2.8.

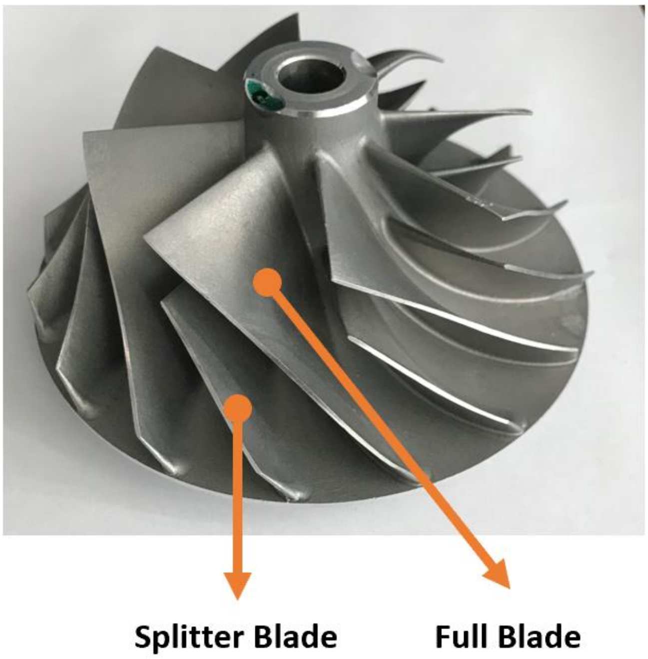

Figure 2. 8 Centrifugal compressor full and splitter blades

Splitter blades are often used to reduce vane blockages, increase the compressor choke flow range and increase the overall compressor flow range. In addition, the design of the splitter blades may be the same as the full blades or they have a completely different structure.

2.2.3 Diffuser

The diffuser leaves a large space, reducing the flow of the air that leaves the compressor and reaches high speed. The absolute spreading area velocity value of the flow leaving the compressor wheel is higher than the normal velocity.

Diffusers are used in a variety of ways. It is a vaneless diffuser which is generally simple and suitable for commonly used small compressors. It is another type of diffuser used in vaned diffuser. Vaned diffusers are divided into two as channel type and airfoil type.

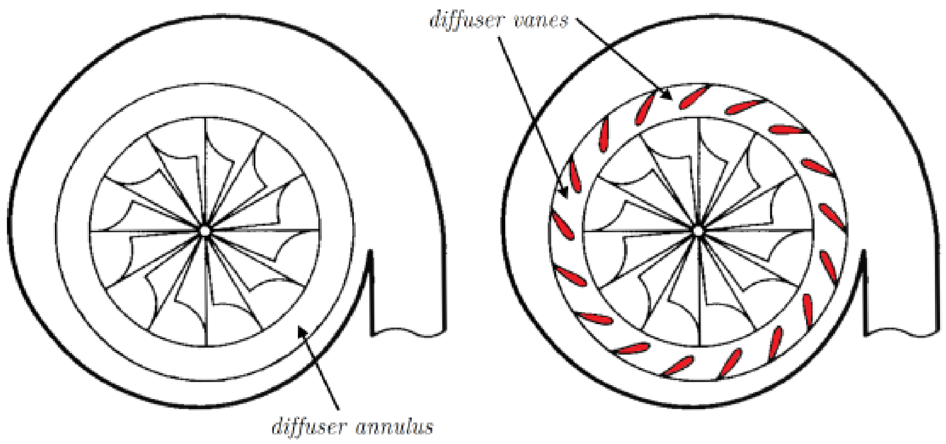

Figure 2. 9 Configurations of diffusers: vaneless (left) vaned (right) [19]

At the high-pressure ratios (2.5<PR<4.0), mechanical stresses occur in the compressor part. These strains occur both in the diffuser and in the compressor blades. The diffuser used consist of two types as in Figure 2.10, with and without blades.

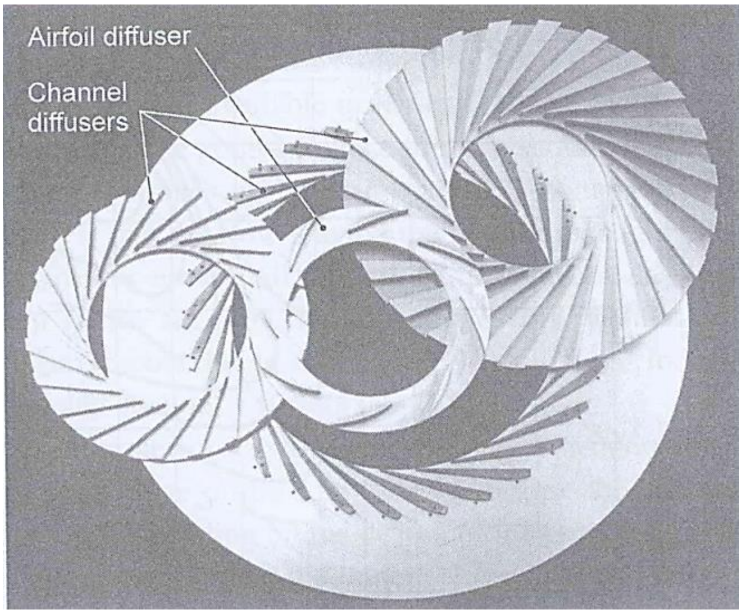

Figure 2. 10 Airfoil diffuser types [19]

Another issue to consider in diffuser design is the stability of the flow. While providing static pressure recovery by converting kinetic energy in diffuser, attention must be taken not to destabilize the flow.

2.2.4 Volute

The volute is the structure that transmits the flow from the diffuser to the outlet pipe. It usually has an increasing circular cross section towards the exit and is formed by rotating this section 360° around the diffuser. Similar to diffuser, the kinetic energy of the flow is converted into pressure with the increasing are in the volute, resulting in an increase in static pressure. One of the most important points in volute design is the tongue part of the volute. In the place where the volute makes a full turn around the diffuser and joins with the outlet pipe, there is a part called the tongue that connects the beginning and the of the volute.

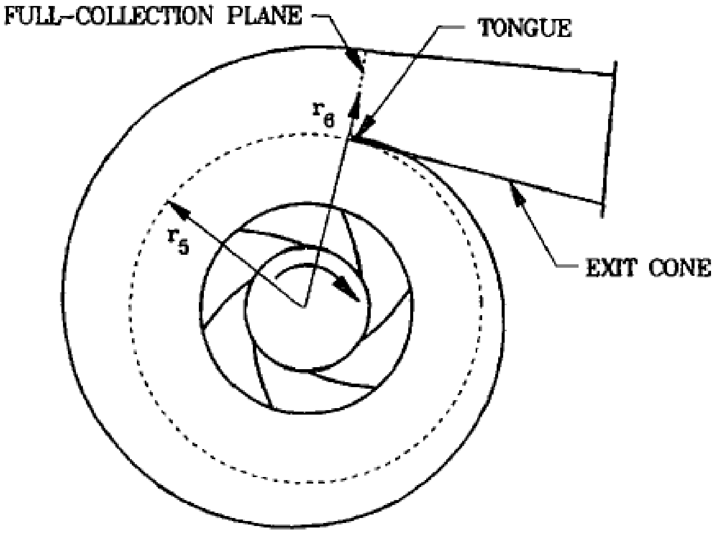

Figure 2. 11 Volute nomenclature [18]

If the tongue design is not good, flow separations occur at this point, some of the flow that should pass from the volute to the outlet pipe is directed towards the diffuser, changing the pressure and velocity distribution, causing a decrease in efficiency.

2.3 Compressors Thermodynamics

Thermodynamic examination of compressor is very necessary in revealing the operating logic of the compressor and evaluating its performance. In particular, when examining the efficiency issue, it is necessary to know the thermodynamic properties of the compressor. In this section, compressor thermodynamics are mentioned.

2.3.1 First Law of Thermodynamics for the Compressor

The first law of thermodynamics states that energy cannot be created out of nothing, but it states that it can change form. This law is also known as the “conservation of energy principle”.

In compressors, which are accepted as continuous flow open systems, “the total mass in the control volume does not change with time” [19]. Therefore, as expressed in Equation 2.1, the total mass leaving the system and the total mass entering the system are equal. This is called the principle of conservation of mass.

$$\sum \dot{m}_{in} = \sum \dot{m}_{out} \tag{2.1}$$

In systems where the mass entering and leaving the control volume in unit time is equal, the mass flow rate ($\dot{m}$) is more important than input and output. Since compressors usually have one inlet and one outlet, the equation can be reduced to 2.1. If the mass flow rate is expressed in terms of density (ρ), velocity (V) and area (A), the equation becomes 2.2. Here, velocity is the average in flow direction and area is the cross-sectional area perpendicular to the flow direction.

$$\dot{m}_{in} = \dot{m}_{out} = \dot{m} = (\rho \mathrm{VA})_{in} = (\rho \mathrm{VA})_{out} \tag{2.2}$$

In continuous flow open systems, the total energy of the control volume remains constant, similar to the fact that the mass of the control volume does not change. Therefore, the energy entering the control volume as mass, heat or work is equal to the energy released [19]. If the Equation 2.2 is also written for energy, Equation 2.3 is obtained.

$$\Delta E_{System} = \sum E_{out} - \sum E_{in} \tag{2.3}$$

For an open system with continuous flow, the first law of thermodynamics [19] is written as follows:

$$\dot{Q} - \dot{W} = \sum \left(\dot{m} \left(h + \frac{V^2}{2} + gz \right) \right)_{out} - \sum \left(\dot{m} \left(h + \frac{V^2}{2} + gz \right) \right)_{in} \tag{2.4}$$

For continuous flow open systems with one inlet and one outlet, such as compressors, the equation is reduced to 2.5.

$$\dot{Q} - \dot{W} = \dot{m} \left[h_{out} - h_{in} + \frac{{V_{out}}^2 - {V_{in}}^2}{2} + g(z_{out} - z_{in}) \right] \tag{2.5}$$

Here, $\dot{Q}$ is the heat exchange between system and the environment per unit time. If there is heat transfer from the system to the surroundings, this term is negative. The power per unit time is denoted by "$\dot{W}$". Unit for machines such as compressor and pumps power in time represents the mile work per unit time. “g" is gravitational acceleration and “z” is the height. It can also be written as the potential energy signifies the change; $g(z_{out}$ -$z_{in})$ =Δpe. In turbomachines such as compressor and turbines, this term is often neglected because the height difference between the inlet and outlet is very small. The kinetic energy change is expressed as $({V_{out}}^2 - {V_{in}}^2)/2 = \Delta ke$. Since the effect of kinetic energy change on the system is proportional to the square of the speed, this term should not be neglected in high-speed compressor where the speed difference between inlet and outlet is large. h_{out} - $h_{in} = \Delta h$ represents the enthalpy differences between inlet and outlet. For ideal gases, the enthalpy change is written as in Equation 2.6, where "$C_{p,avg}$" is the mean specific heat at constant pressure. This term cannot be neglected as the work done by the compressor is directly related to the enthalpy difference between the inlet and outlet.

$$\Delta h = C_{p,avg}(T_{out} - T_{in}) \tag{2.6}$$

2.3.2 Second Law of Thermodynamics for the Compressor

Clausius states the second law of thermodynamics as “it is impossible for a machine working by performing a thermodynamic cycle to take heat from low-temperature body and give it to a high-temperature body without any other energy interaction [19]. In other words, the thermal efficiency of no machine is 100 percent.

With the second law of thermodynamics, the concepts of entropy and reversible work emerged. Entropy, which stands for molecular disorder, is denoted by letter “S" and is expressed as follows:

$$dS = \frac{dQ}{T} \tag{2.7}$$

If a system changes from a regular state to a more disordered state, it’s entropy will increase. The concept of reversible work (W_{tr}) is the maximum useful work that can be taken from that system while the process is takin place in the system [4]. If a process is reversible, the entropy production will be zero. In other words, the entropy production in a process change is directly proportional to the irreversibility of that process.

The second law of thermodynamics can be written as follows for a continuous flow open system with "T_0" ambient temperature, "s" specific entropy, "$\dot{S}$" total entropy production of the system.

$$\dot{S} = \sum(\dot{m}s)_{out} - \sum(\dot{m}s)_{in} - \frac{\dot{Q}}{T_0} \tag{2.8}$$

Equation 2.5 can be substituted in Equation 2.8 by subtracting the expression "Q". In order to find the reversible work, if it is assumed that the total entropy production is equal to zero and the system consists of one inlet and one outlet, the new version of Equation 2.8 is as follows;

$$\dot{W}_{tr} = \dot{m}\left[(h_{out} - h_{in}) - T_0(s_{in} - s_{out}) + \frac{{V_{in}}^2 - {V_{out}}^2}{2} + +g(z_{in} - z_{out})\right] \tag{2.9}$$

2.4 Compressors Aerodynamics

The flow that develops through the vanes and blade passages transitions is extremely difficult to study due to its instability. Instability is mainly crated by the presence of rotating and stationary devices in close interaction with each other: their effects can be ignored if fixed reference systems are introduced to the component being analyzed (for example, the impeller).

Figure 2.12 shows typical flow velocity triangles near blade tip in both leading and trailing edges. In particular, three different velocity vectors can be defined:

C: absolute velocity

W: relative velocity

U: Tangential velocity

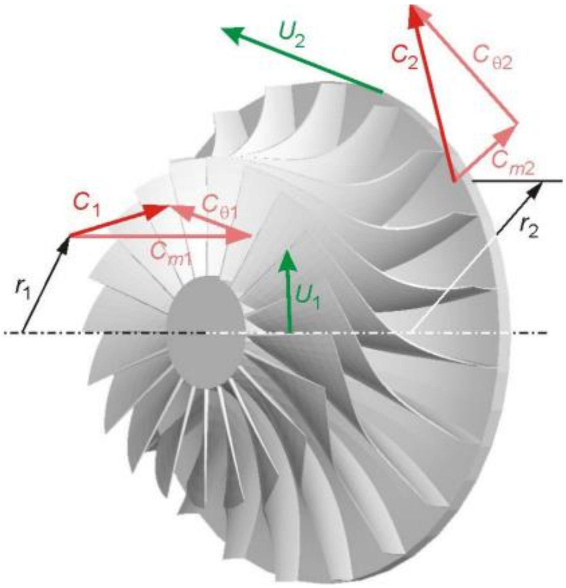

Figure 2. 12 Velocity triangles on radial flow machine [2]

The inlet triangle is defined by inflow parameters and geometrical dimensions on leading edge. If the inlet triangle is need to be examined in detail, Figure 2.13 should be studied. As indicated in the figure, the differences between selected blade angle "β_{1B}" and flow angle "β_1" is called as the angle of incidence.

$$i = \beta_{1B} - \beta_1 \tag{2.10}$$

Here;

β_{1B}: Blade angle

β_1: Fluid angle

$$U = 2\pi r N \tag{2.11}$$

$$C_m = \frac{\dot{m}}{A\rho_f};\ A_f = C_D \pi (r_t^2 - r_h^2);\ C_D = 1 - B_1 \tag{2.12}$$

Here, "B" represents the boundary layer blockage and is calculated with $U = 1 - (A_{flow} - A_{geometric})$. In other words, it expresses the blocking effect arising from the difference between the area through which fluid can pass and geometric are of the blade. Ideally, these two areas should be equal to each other, so $= 0$.

"C_D" is the evacuation coefficient and is found by $C_D = 1 - B$. Since $B = 0$, the value of "C_D" is also equal to 1.

$$V_\theta = 0 \tag{2.13}$$

To remember the formula for density;

$$\rho = \frac{P}{RT} \tag{2.14}$$

Pressure and Mach number relation;

$$\frac{P_0}{P} = \left(1 + \frac{\gamma - 1}{2} M^2\right)^{\frac{\gamma}{\gamma - 1}} ; M = \frac{V}{a} \tag{2.15}$$

Temperature and Mach number relation;

$$\frac{T_0}{T} = 1 + \frac{\gamma - 1}{2} M^2 \tag{2.16}$$

$$a = \sqrt{\gamma \mathrm{RT}} \tag{2.17}$$

Calculation of flow velocity;

$$V = \sqrt{C_m^2 + C_\theta^2} \tag{2.18}$$

Calculation of relative velocity;

$$W = \sqrt{(C_\theta - U)^2} + C_m^2 \tag{2.19}$$

$$M_{rel} = \frac{W}{a} \tag{2.20}$$

By means of the above equations, it is possible to calculate the inlet aerodynamic parameters in the initial design of the compressor wheel.

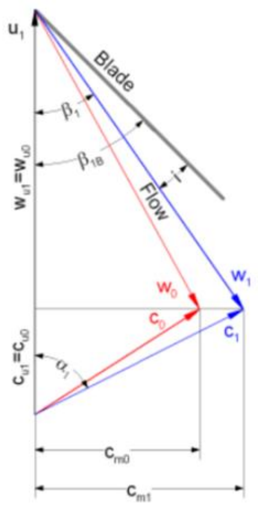

Figure 2. 13 Inlet triangle [20]

The outlet triangle is determined by geometrical dimensions of the flow channel and the selected blade angle "β_{2B}". This area of blade is called as trailing edge. If the outlet triangle is need to be examined in detail see in Figure 2.14. For determination of "β_{2B}" it is important to know the deviation between the flow angle and the blade angle. The relative flow direction "w_2" at impeller outlet dos not exactly follow the blade contour at angle "β_{2B}". The flow angle "β_2" is always smaller than blade angle "β_{2B}" due to the slip velocity. This difference is called deviation angle "δ".

$$\delta = \beta_{2B} - \beta_2 \tag{2.21}$$

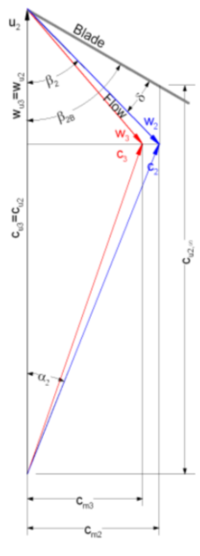

Figure 2. 14 Outlet triangle [20]

The necessary relations for calculating the aerodynamic parameters as at the impeller outlet are given below.

$$\Delta h_0 = U_2 C_{\theta 2} - U_1 C_{\theta 1} \tag{2.22}$$

$$C_{\theta 2} = U_2 + C_{m2} \tan \beta_{2B} - C_{slip} \tag{2.23}$$

Circumferential velocity of compressor is given below;

$$U_2 = 2\pi r_2 N \tag{2.24}$$

$$C_{m2} = \frac{\dot{m}}{\rho_2 A_{f2}};\ A_{f2} = 2\pi r_2 b_2 \tag{2.25}$$

Slip velocity is given below;

$$C_{slip} = U_2(1 - \sigma) \tag{2.26}$$

$$\rho_2 = \frac{P_2}{RT_2} \tag{2.27}$$

$$\Delta h_0 = C_p \Delta T_0 \tag{2.28}$$

2.4.1 Euler Turbomachinery Equation

In the impeller of the radial flow compressor, energy transfer occurs due to rotation of impeller, accompanied by an increase in stagnation pressure and enthalpy of the liquid. By ensuring its efficient diffusion in both impeller and the diffuser, a good compressor stage efficiency can be achieved. The flow Mach number affects diffusion and it is desirable to obtain a minimum relative Mach number at the impeller inducer and a minimum absolute Mach number at the impeller exducer.

Euler work is known as this primary soured of energy input and it is the basis for calculating work input in compressors. The total torque required to start the compressor is expressed in equation 2.29.

$$\mathrm{T_c} = \dot{m}(\mathrm{C}_{W2}\mathrm{r}_2 - \mathrm{C}_{W1}\mathrm{r}_1) \tag{2.29}$$

This assumes that the fluid entering and leaving the impeller condenses at radii "r_1" and "r_2", respectively and operates in steady state. In turbocharging work, the Euler equation is usually expressed in 2.30.

$$\Delta\mathrm{T_c} = \frac{\mathrm{C}_{W2}\mathrm{r}_2 - \mathrm{C}_{W1}\mathrm{r}_1}{\mathrm{C}_p} \tag{2.30}$$

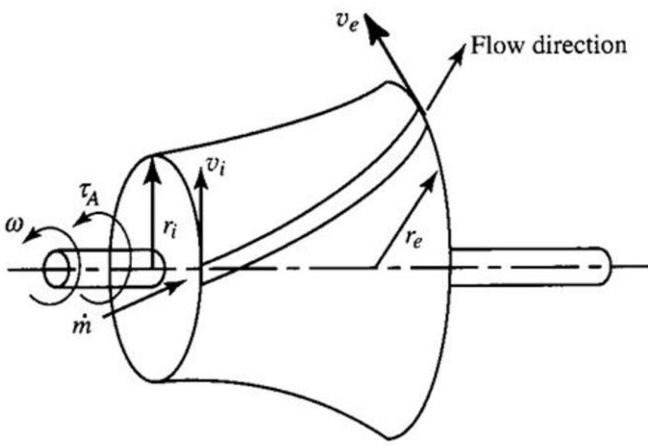

Figure 2. 15 Display of speed and torque in a turbomachinery system [21]

2.5 Compressors Performance

In this section, terms that are frequently mentioned when evaluating compressor performance and conditions that affect performance are discussed.

There are 4 main parameters that determine the performance of compressor. These are compression ratio, isentropic efficiency, corrected flow and corrected shaft speed. Figure 2.16 shows the schematic diagram of a compressor.

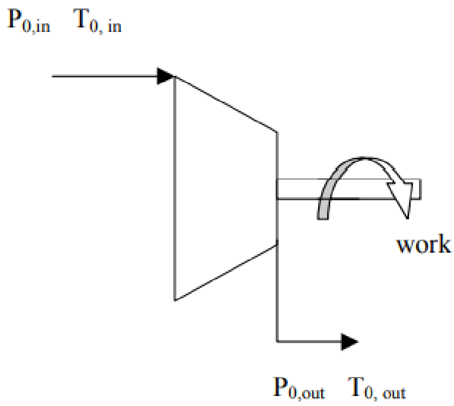

Figure 2. 16 Compressor schematic [7]

As can be expected, the compression ratio is the ratio of the pressures of the air entering the compressor and being pressurized there and sent from the engine. The isentropic efficiency is the impeller efficiency for that no heat exchange condition. Flow rate is the flow rate entering the compressor and shaft speed is the number of revaluations of the common shaft.

2.5.1 Compressor Map

Each compressor has a compressor map that includes all these parameters and determines the characteristics of the compressor. Below is an example of this compressor map.

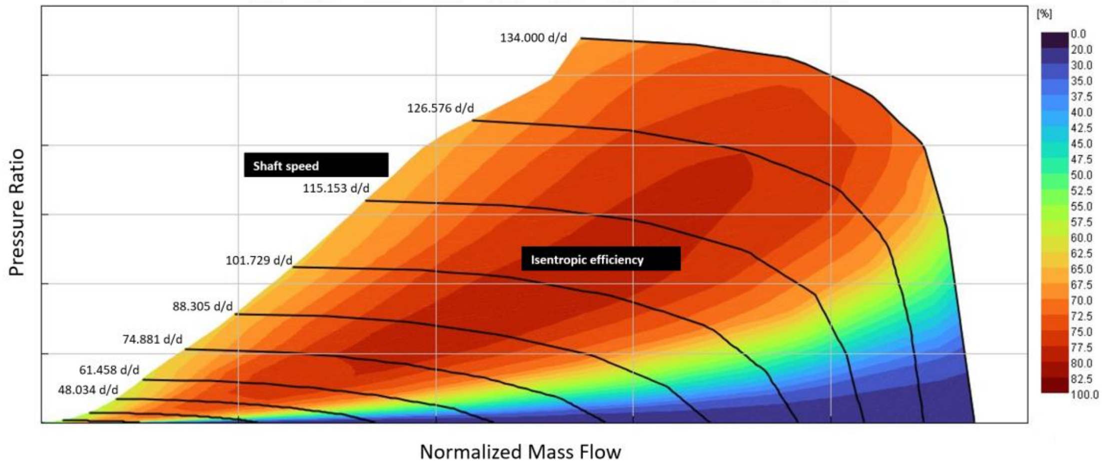

Figure 2. 17 Compressor map characteristic

The X-axis of the map shows the air flow and the Y axis the pressure ratio. In the map, there are near-horizontal constant shaft velocity lines and isentropic efficiency islands. Also, the regions of the map can be seen in the Figure 2.18.

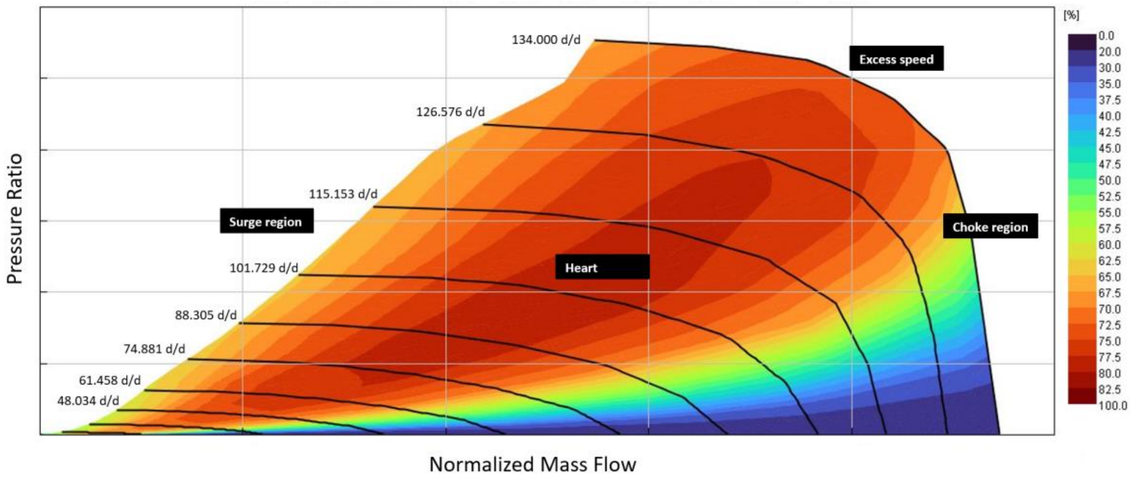

Figure 2. 18 Regions of compressor map

The map consists of 4 main areas: the surge region, the choke region, the excess speed region and the heart.

The unstable operating region (surge) is the most important region that adversely affects the strength of the compressors. The compressor is requested to work as far away from this area as possible. As can be seen from the map, the surge region corresponds to the low air flow, high pressure ratio region. Serious air flow and pressure fluctuations occur in a compressor that is intended to be operated in this area and the compressor enters an undesirable cycle. In extreme cases, it is also observed that backflow occurs in the compressor wheel. In order to prevent this event, the compressor inlet directions that can provide smooth entry to the blade angles are determined. Figure 2.19 shows how surge occurs.

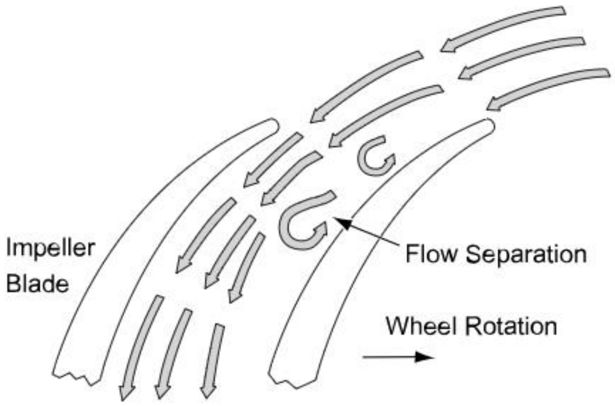

Figure 2. 19 Surge [22]

The surge is an effect experienced in the engine low end speed. For this reason, the torque curve at low engine speeds cannot be improved at desired level. The factor limiting this curve to be pulled up at low speeds is the surge event that occur the compressors.

Choke limit is the event that the velocity of the gas flow in the narrowest space between the blades exceeds the speed of sound. In this case, although the compressor speed increases, the flow volume does not increase. Figure 2.20 shows how choke occurs.

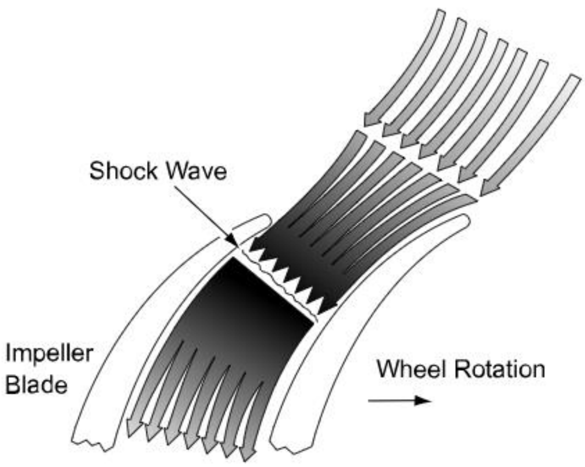

Figure 2. 20 Choke [22]

The excess speed region and the choke region are usually close to each other. The excess speed region indicates the maximum allowable speed of the turbocharger system shaft and this limit is a limit created by mechanical limitations and it is desired that the turbochargers system stays away from this upper shaft speed limit. It is a region that needs attention and stay safe, especially in engines operating at high altitudes.

The heart region is the area where the compressors is isentropically most efficient. The operating curve of the compressor is desired to be as close to this region as possible. In this way, an increase in performance and efficiency is achieved.

During the matching operation, attention should be paid to compressor map regions mentioned above. The range of engine operating points on a compressor is shown in Figure 2.21.

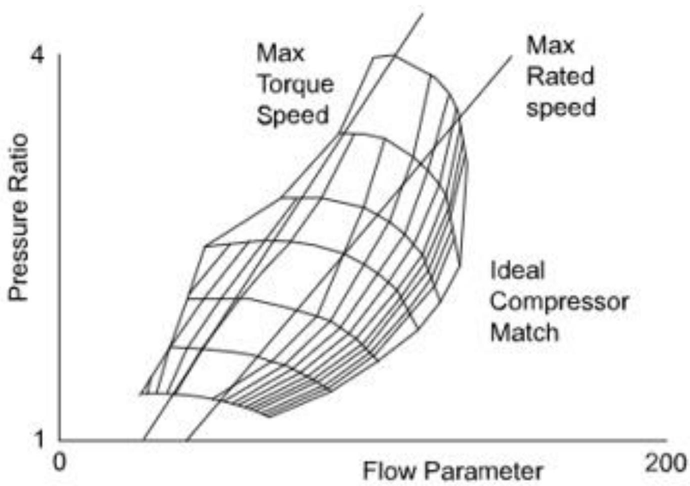

Figure 2. 21 Ideal compressor operating zone [22]

As a result of the first matching study, the compressor size to be required later should be interpreted according to the region studied on the map. Compressor size based on engine operating conditions can be interpreted as shown in Figure 2.22.

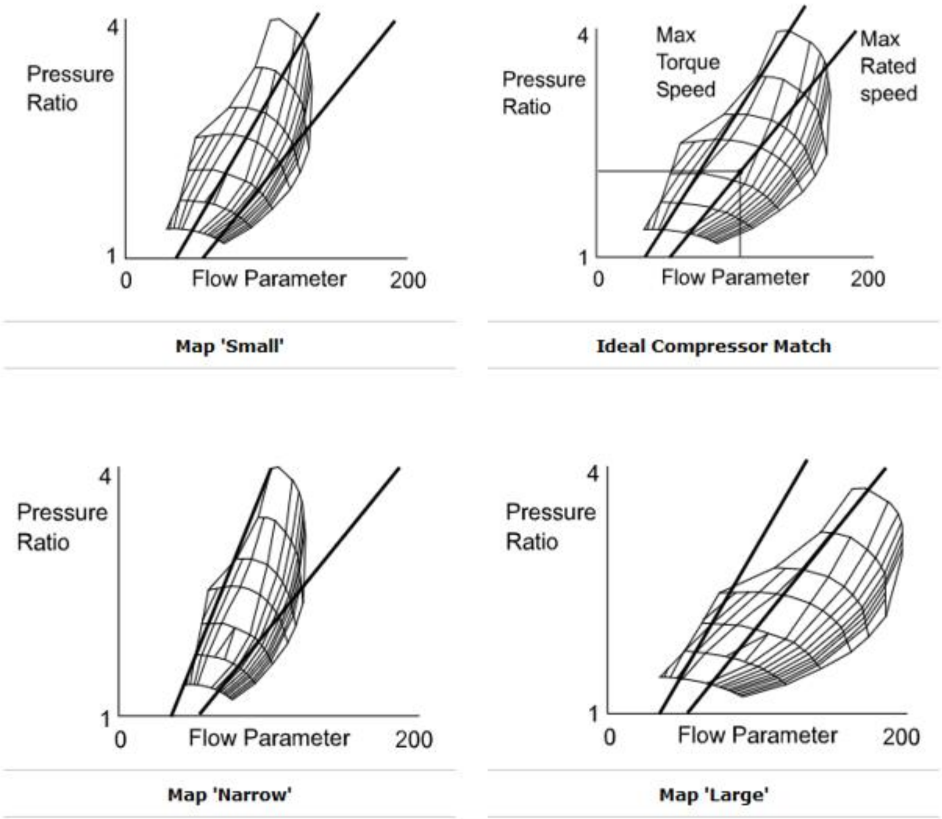

Figure 2. 22 Interpretation of compressor size operating zone [22]

2.5.2 Efficiencies

The efficiency of the compressor can be expressed as the ratio of the ideal energy change to the actual energy change. Since compressors are power consuming machines, the ideal energy change means the least possible energy change. Two kinds of efficiencies will be the focus of this chapter. There are the isentropic and polytrophic processes.

- **Isentropic Efficiency**

In the definition of isentropic efficiency, the assumption is made that the ideal energy change is an isentropic process. The isentropic process is adiabatic and internally reversible.

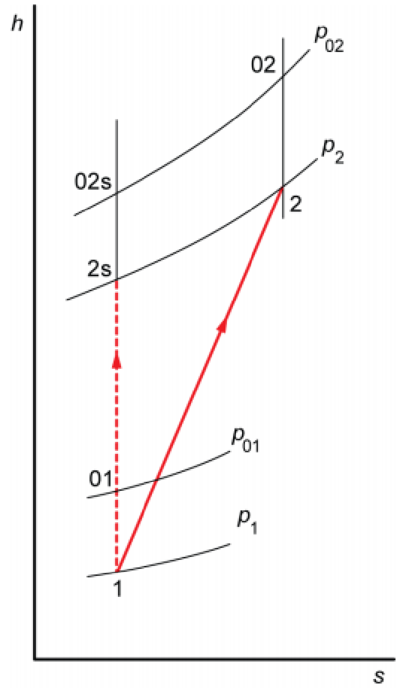

Figure 2. 23 Isentropic process [2]

The total-to-total isentropic efficiency is expressed:

$$\eta_{tt,c} = \frac{h_{02s} - h_{01}}{h_{02} - h_{01}} = \frac{(p_{02}/p_{01})^{(k-1)/k} - 1}{(T_{02} - T_{01}) - 1} \tag{2.31}$$

The total-to-static isentropic efficiency is expressed:

$$\eta_{ts,c} = \frac{h_{2s} - h_{01}}{h_{02} - h_{01}} = \frac{(p_2/p_{01})^{(k-1)/k} - 1}{(T_{02} - T_{01}) - 1} \tag{2.32}$$

- **Polytrophic Efficiency**

The polytrophic efficiency is assumed to be a polytrophic process of ideal energy exchange. An expression for the polytrophic efficiency can be expressed in equation 2.33.

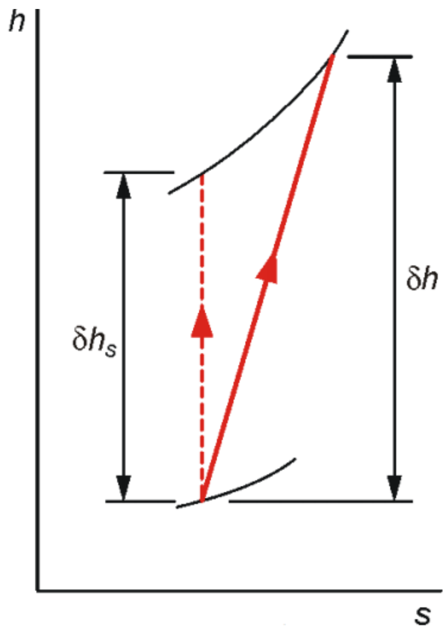

Figure 2. 24 Polytrophic process [2]

$$\eta_{p,t-t} = \frac{ln(p_{02}/p_{01})^{(k-1)/k}}{ln(r_{02}/r_{01})} \tag{2.33}$$

2.5.3 Losses

In this section, the factors called compressor losses, which adversely affect the compressor performance and cause the compressor efficiency to decrease, are discussed.

- **The Slip (Deviation) Factor**

The angle difference between the blade angle at the outlet end of the blade and the flow angle is called the deflection angle at the outlet. The deflection angle causes the tangential component of the absolute velocity at the outlet to be smaller. As a result, the losses increase and the power transferred to the fluid decreases.

The slip factor (σ) is used to examine the effect of the deflection angle on the compressor. The slip factor was defined by Dixon as the ratio of the tangential component of the absolute velocity of the flow actually occurring at the impeller exit to the tangential component of the ideal absolute velocity. If this value is equal to 1, it represents the ideal situation with no slip.

$$\sigma = \frac{C_{\theta 2}}{C_{\theta 2}{}'} < 1 \tag{2.34}$$

There are a variety of slip factor correlations available, but the principal characteristic and options can be illustrated by presenting those of Wiesner (1967). Wiesner slip factor correlation is a function of blade number and blade backsweep angle. The Wiesner slip factor correlation is given by the equation 2.17. Slip velocities "c_s", required for the calculation of the non-design slip factor, it can come from 1D two-zone calculations or it can come from 3D CFD viscous calculations that provide a mass-averaged values for "c_s".

$$\sigma = 1 - \sqrt{cos\beta_{2b}} \Big/ Z_R^{0.7} \text{ (meridional angle system)} \tag{2.35}$$

When we express the σ with $\overline{c_s}$;

$$\sigma = 1 - \frac{\overline{c_s}}{u_2} \tag{2.36}$$

And;

$$\overline{c_s} = u_2 + \overline{c_{m2m}}\tan\beta_{2b} - \overline{c_{\theta 2m}} \tag{2.37}$$

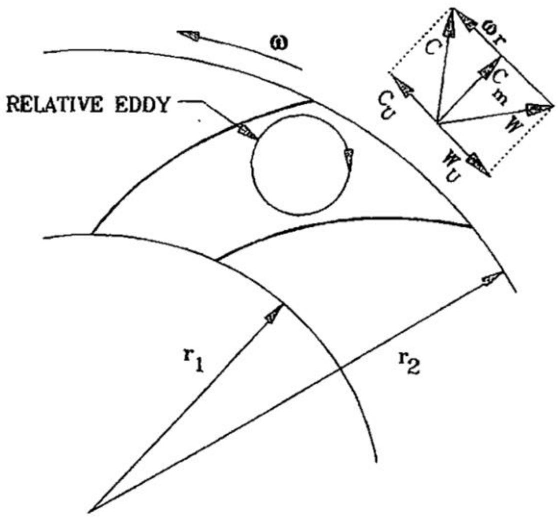

Figure 2. 25 The concept of slip factor [2]

Wiesner slip factor correlation is a defined function of compressor wheel design parameters which are blade outlet backsweep angle "β_{2b}" and total number of blade "z". You can also see the graph that Japikse shows the effect of the above-mentioned combination on slip factor.

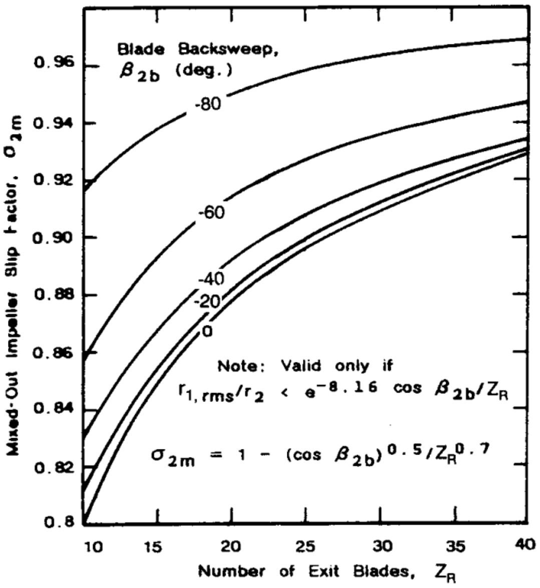

Figure 2. 26 Wiesner slip factor correlation with blade backsweep and blade number as parameters [2]

Using the impeller two-zone approach, the tangential exit velocities and the slip factor mainly depend on the predefined deviation angle of the primary and secondary flow and the magnitude of the diffusion rate.

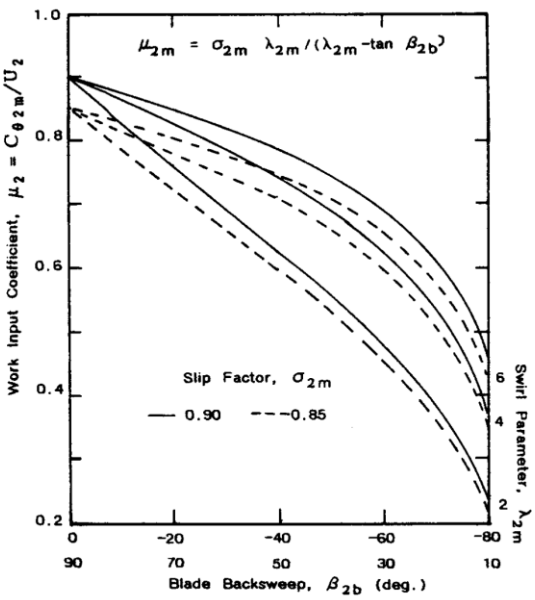

Figure 2. 27 Work input coefficient change on slip factor with backsweep [2]

- **The Relative Eddy Concept**

Dixon mentioned that suppose an irritation-free and frictionless fluid flow is possible through an impeller. If the rotation of the absolute flow at the outlet is still zero, the absolute flow must have entered the impeller without rotation. The angular velocity of the fluid relative to the impeller is “Ω” because the impeller itself has an angular velocity “Ω”. This is called the relative vortex Figure 2.28 (a).

At the exit of the impeller, the relative flow can be regarded as a flow onto which a relative vortex is added. The mean relative flow from the impeller passages is at angle to the blades and in the opposite direction to the blade movement, and the net effect of these two movements is shown in Figure 2.28 (b). This is the basis of various early slip theories.

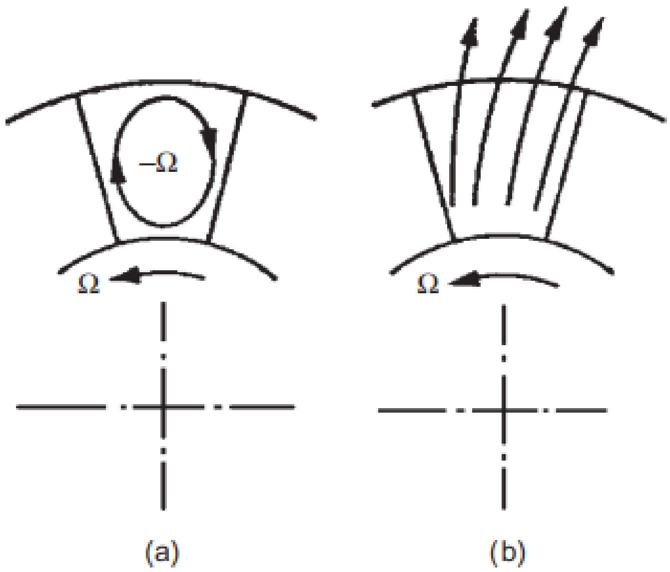

Figure 2. 28 (a) Relative eddy without any through-flow; (b) the relative flow at impeller outlet (through-flow added to relative eddy) [27]

- **Friction Losses**

Friction loss occurs as a result of the non-slip principle between the flow and the surface. There are many types of friction that cause losses inside the compressor. Since there is a long and undirected flow path in vaneless diffusers, the losses due to surface friction are high in this type diffusers.

Since there is no blade tip gap in closed impellers, blade tip leakage losses are prevented, but it brings an extra surface compared to open type impellers, therefore surface friction increases. The first reason for this is the decrease in the area that the flow can pass at the impeller inlet with the increasing number of blades, the increase in the flow velocity and the increase in the Reynolds number. The second reason is that the friction surface increases with the increase in the number of blades.

- **Blade Tip Leakage Losses**

Blade tip leakage losses occur only in open impellers blade tip clearances. The event that the flow passes from the high-pressure side of the blade to the low-pressure side (suction side) due to the gap at the tip of the blade is called blade tip leakage. This leakage causes losses in compressor efficiency. Japikse stated that it the blade tip clearances increases by 3% of the blade tip width, the efficiency decreases by 1%.

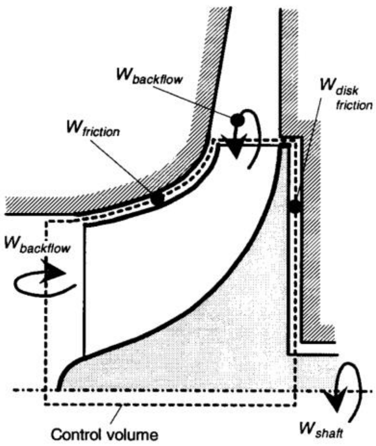

Figure 2. 29 Work transfer [2]

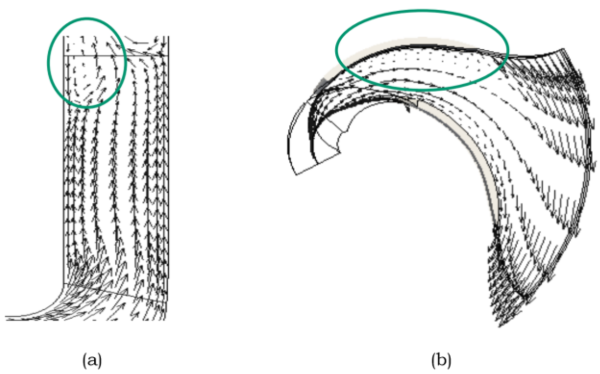

Figure 2. 30 Velocity vector on meridional plane (a), velocity vector on blade-blade plane [2]

3
3D CFD ANALYSIS OF EXISTING COMPRESSOR

In this section, the method followed in numerical analyzes to examine the effect of impeller design parameters on compressor efficiency is explained in detail. In addition, the geometry of the existing compressor has been examined. Three different operating points were determined on the compressor map provided by the supplier. The compressor was verified by performing three-dimensional computational fluid dynamic (CFD) analyzes at the determined operating points.

3.1 Existing Compressor Geometry and Experiment Data

The three-dimensional geometry prepared to use in CFD analysis after undergoing surface cleaning processes. During the surface cleaning processes, critical blade surfaces were not interfered.

The compressor impeller consists of eight main and eight splitter blades. The diffuser is vaneless and radial direction and the height remains constant throughout. The value of the blade tip clearance is somewhere between 0.25 mm and 0.35 mm. Compressor rotates in -Z direction.

3.2 Three Dimensional CFD Analysis

Three-dimensional continuous system CFD analyzes of the compressor geometry were performed using ANSYS CFX. In the mesh generation process, TurboGrid was used for the impeller, and ANSYS Meshing was preferred for the remaining parts. Three-dimensional continuous system CFD analysis consist of the stages of creating the geometry, creating the solution mesh, setting up the model, running the analysis, and evaluating the results, respectively. Compressor geometries, which are geometrically arranged and networked, are sent for analysis after the model set up. After the analysis is complete, the results are thoroughly examined.

3.2.1 Generating the Geometries

While performing the three-dimensional CFD analysis of the compressor, the sector model was used for the impeller geometry. In previous experiences, it has been seen that the difference between the analysis with the sector model and the full blade analysis is less than %1, whereas the full blade analysis requires twice as much solution time than the sector model analysis. Therefore, t has been accepted that the sector can be used in the studies within the scope of this thesis. In Figure 3.1, full blade and sector models of the existing compressor wheel, consisting of eight main and eight splitter blades, can be seen.

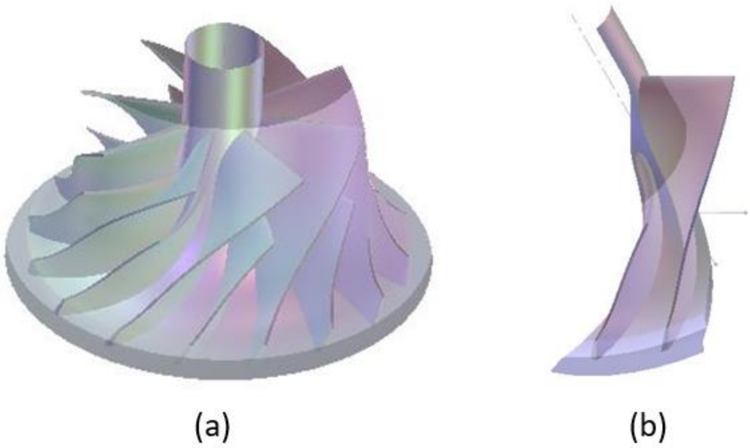

Figure 3. 1 Compressor full blade (a) and sector (b) models.

The effect of compressor the space between the lower surface of the compressor wheel and the diffuser surface on the pressure ratio and efficiency of the compressor was investigated by Tosto, and it was concluded that the amount of fluid remaining in this region is very low, the increase in temperature caused by friction during circulation is also quite local, so it does not seriously affect the performance of the compressor [24]. Therefore, in this study, this gap was removed by following a similar logic, and a smooth transition was achieved from the hub surface to the diffuser surface.

3.2.2 Numerical Producers

The compressor is divided into three as volute, diffuser, and impeller. While the volute and diffuser are fixed, the impeller part has angular velocity because it is a rotating structure.

Again, Tosto performed some analyzes to determine the optimum position of the diffuser and impeller interface and concluded that the optimum position is close to the middle parts of the diffusers, although different diffusers – impeller interface positions do not generally have major effect on the results [23]. In this study, Tosto's work, the diffuser – impeller interface is positioned close to the middle of the diffuser. Since the side of the diffuser close to the diffuser volute is fixed like the volute geometry and a total 3 zones are formed.

While creating the solution network, the total number of cells is around 5.8 million nodes, including inlet duct, wheel (8 main blades + 8 splitter blades), diffuser and volute. These values have been reached by conducting a solution network independence study. Compressor impeller of turbocharger was designed on ANSYS. Vista CCD, BladeGen and TurboGrid tools were used on ANSYS Workbench. Vista CCD is integrated into ANSYS Workbench so that it may be used to generate an optimized 1D (one-dimension) compressor design before moved rapidly to a full 3D (three-dimension) model and CFD (Computational Fluid Dynamics) analysis. 3D CFD analyzes of the compressor geometry were performed using ANSYS CFX, which adopts a finite element based finite volume to solve the Navier-Stokes equations [24]. BladeGen is a geometry creation tool for turbo machinery blades, and it was used to design the 3D model of centrifugal compressor. After creating impeller model, compressor wheel mesh is generated. In the mesh generation process, TurboGrid, which provides high quality hexahedral meshes for the impellers, and ANSYS meshing for the remaining parts was preferred.

3.2.3 Creating the Ansys Model

3D CFD analysis consists of creating the geometry, creating solution mesh, and setting up the model, running the analysis, and evaluating the results, respectively. Air was used as the fluid in the analysis and ideal gas was assumed. SST (Shear Stress Turbulence) was chosen as the turbulence model [25]. Two interfaces are defined, one between the inlet and the impeller and the other between the impeller and the volute. In steady state flow system analysis, it was observed that the frozen rotor model (Multiple Reference Frame MRF) as an interface option gave result closer to the experimental data compared to the mixing-plane type [26]. To better simulate the real simulation as a boundary condition, the total pressure and total temperature were defined at the inlet and the mass flow rate at the outlet. In addition, since the sector model is used for the impeller geometry, periodic boundary conditions are placed on the sides of the flow path. Since the region where the wheel is located is the rotating region, the rotating effect here is obtained by defining the angular velocity value to that region.

3.3 Analysis of Existing Compressor

In this section, validation of the existing compressor with three-dimensional CFD analysis is discussed. In order to achieve this, three different operating points were selected from the performance map of the compressor, and the error rates between the experimental data and the analysis results were calculated after the numerical analysis.

3.3.1 Selection of Operating Points

The compressor map provided by the supplier was used to validate the existing compressor with three-dimensional CFD analysis. For this purpose, three different operating points were determined on the compressor performance map, please see Figure 3.2. The first operating point is close to the surge limit at low end speed region because turbocharger efficiency at low end engine speeds is important to provide the required performance for vehicle. The second operating point is close to maximum efficiency area of map (compressor heart). The third operating point is chosen to be close to the excessive speed limit. Together they cover interesting portions of the compressor map. At each determined operating point, three-dimensional continuous flow system CFD analyzes of the compressor were carried out. The Figure 3.2 shows the performance map of the compressor. The "X axis" represents the normalized mass flow rate, and the "Y axis" represents the pressure ratio. In addition, colored areas represent efficiency.

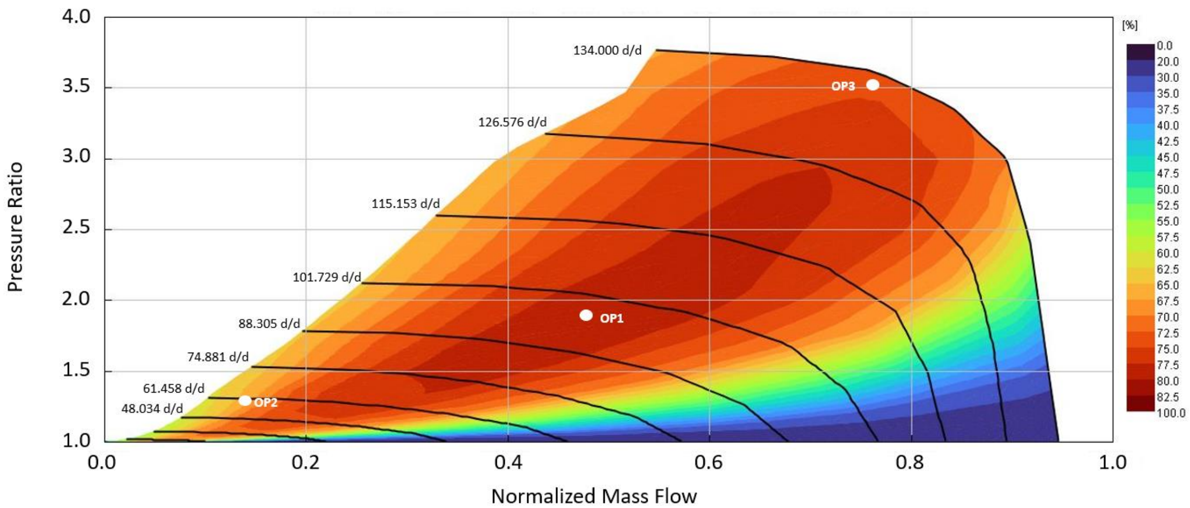

Figure 3. 2 Selected operating points (OP) on compressor map

3.3.2 Evaluation of Results

The pressure ratio and isentropic efficiency values of the compressor obtained as a result of the analyzes made at selected operating points were compared with test data. When these analysis results were compared with the test results of the existing compressor, it was seen that the efficiency error rates between the analysis and the experiment data were %1.6 (OP1), %0.9 (OP2) and %3.1 (OP3). This proves that our CFD model was validated based on the experiment results.

The optimization studies described in the following sections are based on the existing compressor geometry.

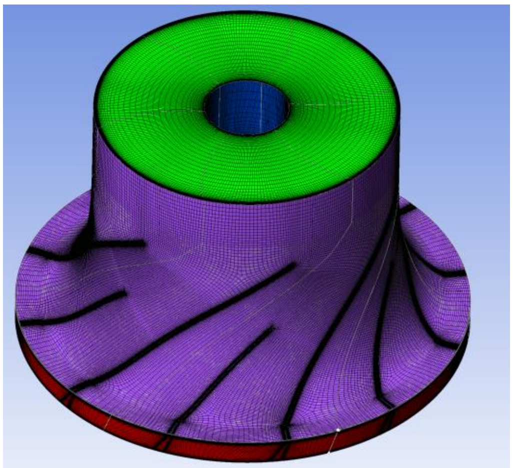

Figure 3. 3 Compressor wheel mesh - ANSYS

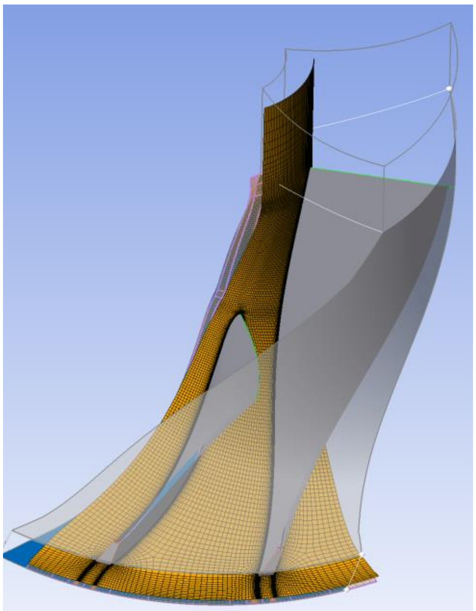

Figure 3. 4 Compressor wheel mesh grid - ANSYS

4
NEW CENTRIFUGAL COMPRESSOR DESIGN

One of the most important turbocharger parts for the performance is compressor wheel. Compressor section of turbocharger system, which was supplied from a turbocharger supplier, was investigated. The efficiencies were found to be low in the compressor performance map provided by the supplier. This paper focuses on improving the efficiency of a centrifugal compressor at the same condition for selected operating points.

To make improvements in the compressor wheel, first of all, the parameters affecting the design of the impeller should be known. And also, as mentioned in the losses section in section 2.4.3, the slip factor plays an important role in the design of the impeller to achieve an efficient system. And based on Wiesner's correlation, we mentioned that the slip factor depends on the total number of blades and the outlet backsweep angle of the blade. In this section, the parameters that has an active role in the design of the compressor wheel are discussed. Literature studies evaluating these parameters are included. In some cases, the new design was shaped based on these literature studies.

4.1 Design Parameters Affecting the Slip Factor on Centrifugal Compressor Design

4.1.1 Total Number of Blades

The first of the most important parameters in centrifugal compressor impeller design is the total number of blades. In some applications, the number of blades can be up to 30. As mentioned before, all the blades of the compressor wheel can be full blades and some of the blades can be composed of splitter blades. Too many blades cause blockages at the impeller inlet. It can bring the compressor to the surge limit earlier. A small number of blades may be insufficient to provide the required pressure ratio.

Busemann and Lewis showed a relationship in the below Figure 4.1 for the variation of the slip factor according to the number of blades of the impeller and the inlet-outlet diameter ratio. As the total number of blades were increased, the slip factor was increased also. As we mentioned in section 2.5.3 of this thesis, the slip factor is loss for compressor.

In this thesis, three different states have been created for the number of blades: six – six (main blades – splitter blades), seven – seven and eight – eight (original compressor wheel).

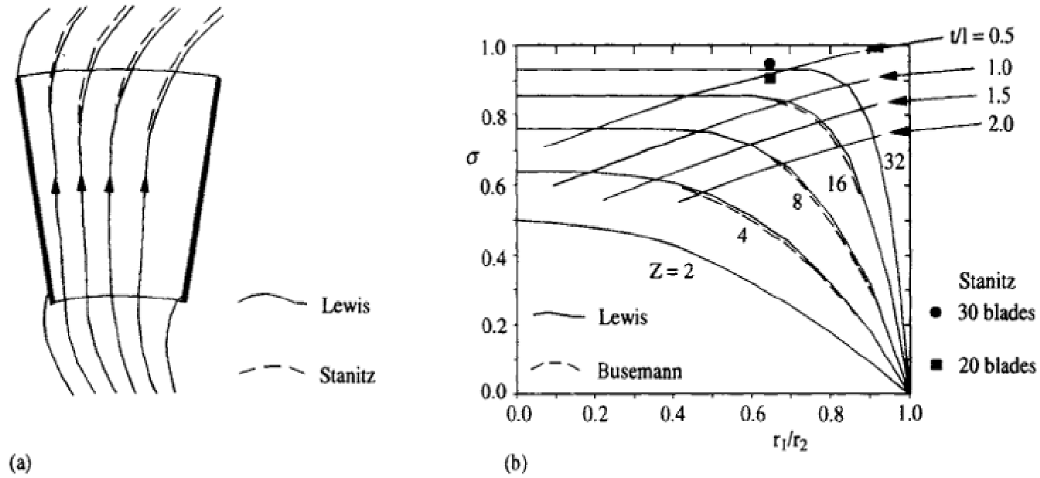

Figure 4. 1 Typical streamline pattern for radial bladed centrifugal impeller and predictions of slip factor for a wide range of geometries and blade numbers: (a) streamline pattern with 20 blades; (b) slip factors for range of geometries [16]

4.1.2 Blade Outlet Backsweep Angle

Compressor blade properties should be well known in order to achieve desired high efficiency and high pressure. Lieblein carried our systematic wind tunnel investigations on the swirl change properties of the profiles of the NACA 65 series. The meaning of the used entities is given following Table 4.1.

Table 4. 1 Blade properties

Symbols	Explanations
l/t	Solidity (chord length/pitch)
β	Angle of relative flow
β_B	Blade angle
u	Circumferential velocity
w	Relative velocity
i	Incidence angle $i = \beta_{1B} - \beta_1$
δ	Deviation angle $\delta = \beta_{2B} - \beta_2$

And also, representations of those symbols on the blade can be seen in Figure 4.2.

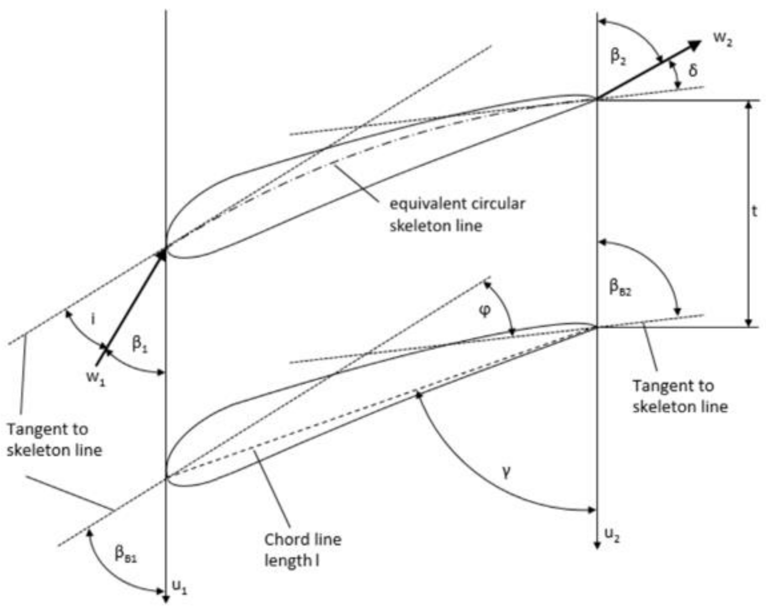

Figure 4. 2 Blade properties [20]

The blade outlet backsweep angle, which is one of the most important parameters of the impeller design, generally remains constant throughout the blade width. The use of backsweep blades at the trailing edge of the impeller will reduce the tangential component of the absolute velocity, which will reduce the work absorption capacity of the impeller. On the other hand, it will achieve higher pressure ratios at low flows. Also, using backswept blades will also result in higher efficiency. The change of velocity triangles in case of using backswept on trailing edge of the blade is shown in Figure 4.3. As seen in the velocity triangles, the absolute velocity $C_{\theta 2}$ will also be lower, meaning that the kinetic energy, which is transferred to diffuser, is lower. Thanks to it, higher efficiency will be achieved.

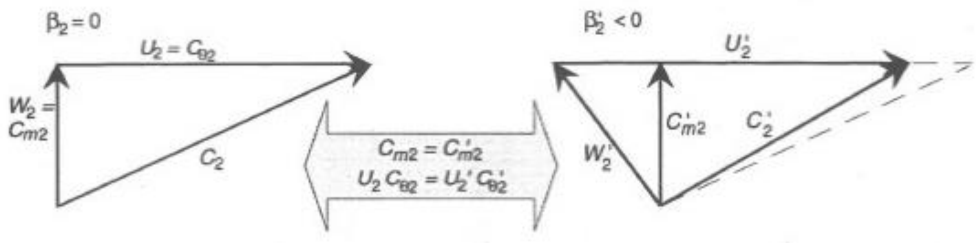

Figure 4. 3 Velocity triangle without backsweep angle (left) and with backsweep angle [2]

The blade outlet backsweep angle is preferred between 30° and 60° in compressor with low speed, as it increases stability and efficiency. However, there is no optimum value range for the blade outlet backsweep angle in the literature, this angle is mostly determined by mechanical limits such as the stress on the blade and impeller and physical limits such as manufacturing capacity [27]. It was mentioned that as the blade outlet backsweep angle increases, the losses will decrease in the diffuser and the efficiency will improve.

Higher work input is desired on compressor design process. Came and Robinson shows blade outlet backsweep angle relation with work factor as shown in Figure 4.4 with total number of blade 18 and the ratio "C_{r2}/U_2 "is 0.2. As seen in graph, work factor decreases when blade outlet backsweep angle increases. In addition, as seen in Figure 4.5 which is with ratio "C_{r2}/U_2 " is 0.2, for compressor with same power, as the blade outlet backsweep angle increases, the peripheral velocity at the outlet will increase, so the stress on the blade will increase [27-28].

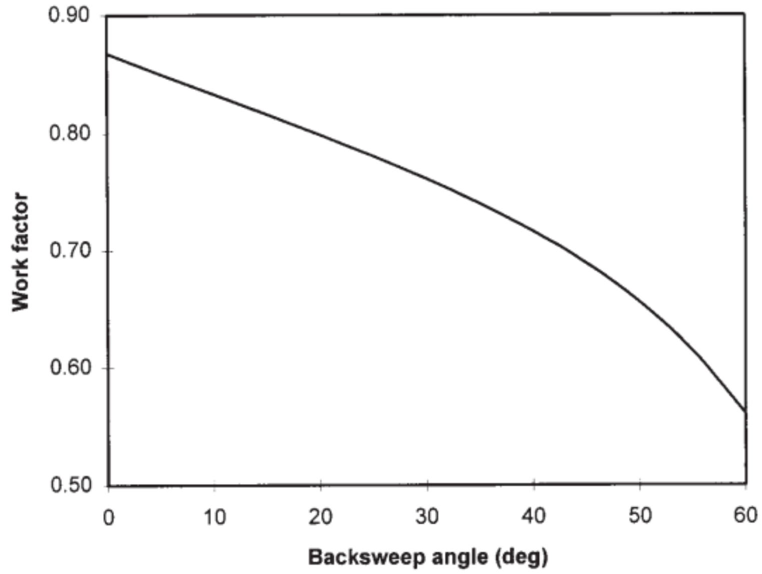

Figure 4. 4 Influence of blade outlet backsweep angle on work [28]

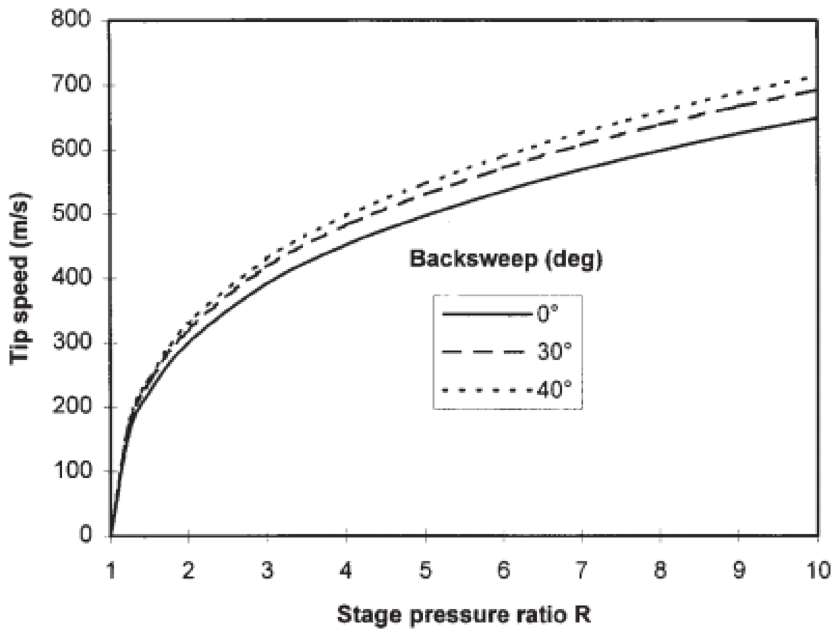

Figure 4. 5 Blade outlet backsweep angle and tip speed relationship [28]

In the study of Hildebrandt and Genrup, the effect of blade outlet backsweep angle and exducer width on flow at the impeller was investigated numerically. Two different blade backsweep angles, 38° (original value) and 45° were used in the study. In Figure 4.6, the total efficiency – reduced mass flow graph of the impeller created according to the analysis results is shown. According to the graph, the highest efficiency value was obtained with the original blade outlet backsweep angle and exducer width. For each fixed blade outlet length, the efficiency decreases as the blade outlet backsweep angle increases. The reason for this is thought to be that the meridional blade length, which increases with the increase of the blade outlet backsweep angle, increases the friction losses.

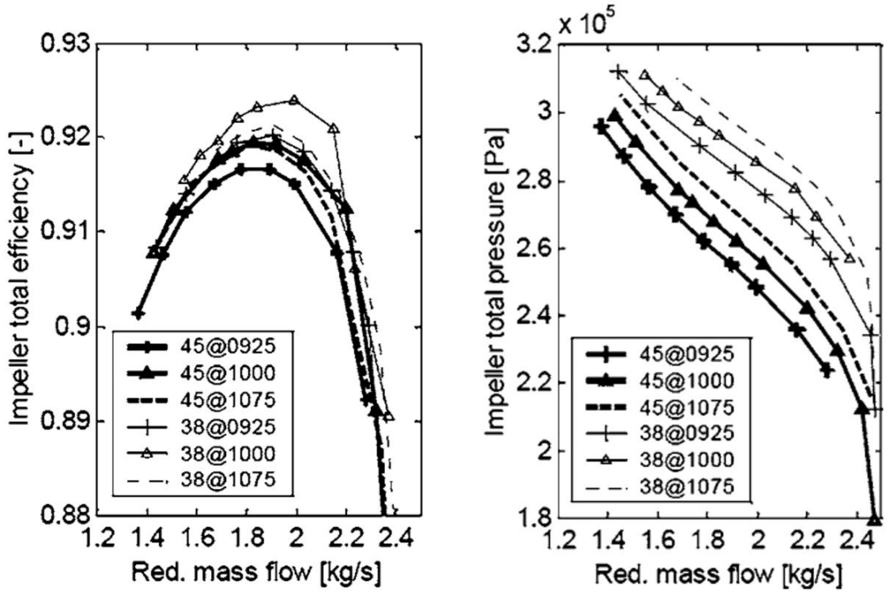

Figure 4. 6 The effect of blade outlet backsweep angle and exducer width on impeller efficiency and total pressure [2]

In this thesis, five different states were presented for the blade outlet backsweep angle (20°, 22.5°, 25° 27.5° (original angle of compressor wheel), and 30°).

5
RESULTS AND DISCUSSION

In this thesis, the turbocharger compressor side, which was tested and has compressor characteristic map, was analyzed. A CFD model was validated against measurements. ANSYS software was used to investigate the flow phenomena with the aim of determining guidelines for CFD model accuracy which would have acceptable differences between measured and analyzed operating points on compressor map. Three different states have been created for the number of blades: six – six (main blades – splitter blades, seven – seven and eight – eight (original compressor wheel). Five different states were presented for the blade outlet backsweep angle (20°, 22.5°, 25° 27.5° (original angle of compressor wheel), and 30°). A total of 45 cases were created as each other combinations for blade number and outlet angle and their effect of them on performance was analyzed for three different operating points. In this section, the analysis results of fifteen different impellers created by changing the impeller design parameters and the new impeller design are mentioned. In addition, a comparison of the existing impeller and the new impeller design has been made.

In the first part, the results of the analyzes that deal with the effects of the impeller design parameters explained in Section 4 on the compressor performance are explained. The effect of parameters in the design of the compressor wheel on the efficiency and pressure ratio of the compressor are investigated. In the second part, the new impeller design determined in line with results in the first part is explained and its differences with existing impeller are mentioned. In the third part, the analysis results of the existing impeller design and the new impeller design are compared. The regions and features developed with the new impeller design are mentioned.

As stated in the sections above, total 45 different analysis iterations, which are combinations of number of blades and backsweep angles were analyzed. Original compressor has 16 blades, 8 of them are splitters blade, and 27.5° backsweep angle. Design iterations are detailed in Figure 5.1.

Operating Point 1 (OP1)		Operating Point 2 (OP2)		Operating Point 3 (OP3)		
Backsweep (β2) Angle	*Number of Blades (Z)*	*Backsweep (β2) Angle*	*Number of Blades (Z)*	*Backsweep (β2) Angle*	*Number of Blades (Z)*	
30	16 Blades	30	16 Blades	30	16 Blades	
27.5	16 Blades	27.5	16 Blades	27.5	16 Blades	Original
25	16 Blades	25	16 Blades	25	16 Blades	
22.5	16 Blades	22.5	16 Blades	22.5	16 Blades	
20	16 Blades	20	16 Blades	20	16 Blades	
30	14 Blades	30	14 Blades	30	14 Blades	
27.5	14 Blades	27.5	14 Blades	27.5	14 Blades	
25	14 Blades	25	14 Blades	25	14 Blades	
22.5	14 Blades	22.5	14 Blades	22.5	14 Blades	
20	14 Blades	20	14 Blades	20	14 Blades	
30	12 Blades	30	12 Blades	30	12 Blades	
27.5	12 Blades	27.5	12 Blades	27.5	12 Blades	
25	12 Blades	25	12 Blades	25	12 Blades	
22.5	12 Blades	22.5	12 Blades	22.5	12 Blades	
20	12 Blades	20	12 Blades	20	12 Blades	

Figure 5. 1 Created 15 different designs on three different operating points (totally 45 different analysis)

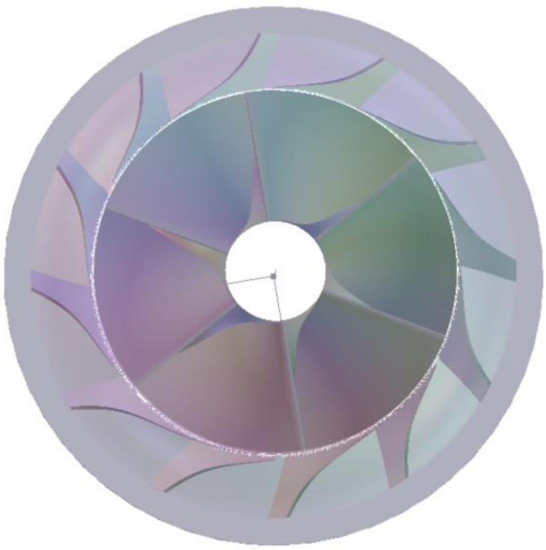

Figure 5. 2 Ansys BladeGen – Wheel 3D model (totally 12 blades)

5.1 Effect of the Blade Outlet Backsweep Angle and the Total Number of Blades on Compressor

In this thesis, turbocharger compressor side, which was tested and has compressor characteristic map, was analyzed. Figure 5.1 details the variation of efficiency and pressure ratio of different backsweep angle and total number of blade combinations. And all combinations were analyzed on three different operating points (45 different cases). The effect of blade backsweep angle and total number of blades on efficiency and outlet pressure are shown at below for three different operating points on compressor map.

The total number of blades is one of the important parameters in impeller design. As explained in detail in section 4.1.1, the desired pressurization may not be achieved in cases where the number of blades is less than necessary, and the total number of blades more than necessary may narrow the throat area at the inlet of the blade and reduce the amount of air that can pass through it. In the graphs below, the effect of the change in the total number of blades of existing compressor on pressure and efficiency can be examined. The blade numbers of the impellers are shown in different colors and line shape on figures. The orange color and square shaped curves represents 16 total number of blades which was the original blade number. The blue and diamond shaped curves represent the 14 total number of blades, respectively, while the gray and triangular curves represent the 12 total number of blades. When the number of blades of the existing compressor wheel, which has sixteen blades, is reduced, the pressure ratio decreases at all three operating points. The biggest reason for this is that the angle of inlet of the low to blade changes with the changing number of blades. As the number of blades increases, it is seen that the pressure ratio increases due to the decrease in the load on each blade, especially as can be seen from Figure 5.3 and Figure 5.7. It has been mentioned that the friction losses will also decrease in the number of blades. In this way, an increase in efficiency has been achieved. However, it should not be forgotten that increasing the number of blades will also change the stress distribution on the impeller, the impeller weight and inertia. In addition, as it can be seen in below figures, since the curve followed by each operating point is different, there will be a different optimum number of blades for each operating point. This is in agreement with Rodgers' work (different optimum blade numbers for different specific speeds) mentioned in literature review in Section 1.

The blade outlet backsweep angle is an impeller design parameter that is especially effective on the efficiency of the compressor. The variation of the blade backsweep angle is shown on the "X-axis" of the graphs, and its effect on pressure and efficiency is also indicated on the "Y-axis". As a result of the analyzes made by changing the blade backsweep angle, it is seen that the efficiency increases up to a point with the decrease in the blade backsweep angle, and then follows an almost constant value. For the third operating point (OP3), the efficiency value started to decrease after a certain blade backsweep angle. The pressure ratio decreases with increasing blade outlet angle, please see to Figure 5.6 and Figure 5.7. As the blade outlet backsweep angle increases, the peripheral velocity at the impeller exit also increases. Increasing the peripheral speed reduces the kinetic energy transferred from the impeller outlet to the diffuser to a certain point, thus converting the more dynamic pressure to static pressure. But this happens up to a certain point because after the optimum blade exit angle, the angle of leaving of the flow from the blade, that is, the losses increase, it can be observed in Figure 5.6, especially. As an end of the evaluation of blade outlet backsweep angle effect on this study, increasing blade outlet backsweep angle will cause a decrease in pressure and efficiency, it has been mentioned by Hilderbrant and Genrup, unlike Japikse. When deciding on the blade backsweep angle, it should be noted that the angle value increases, the stress on the blade will also increase.

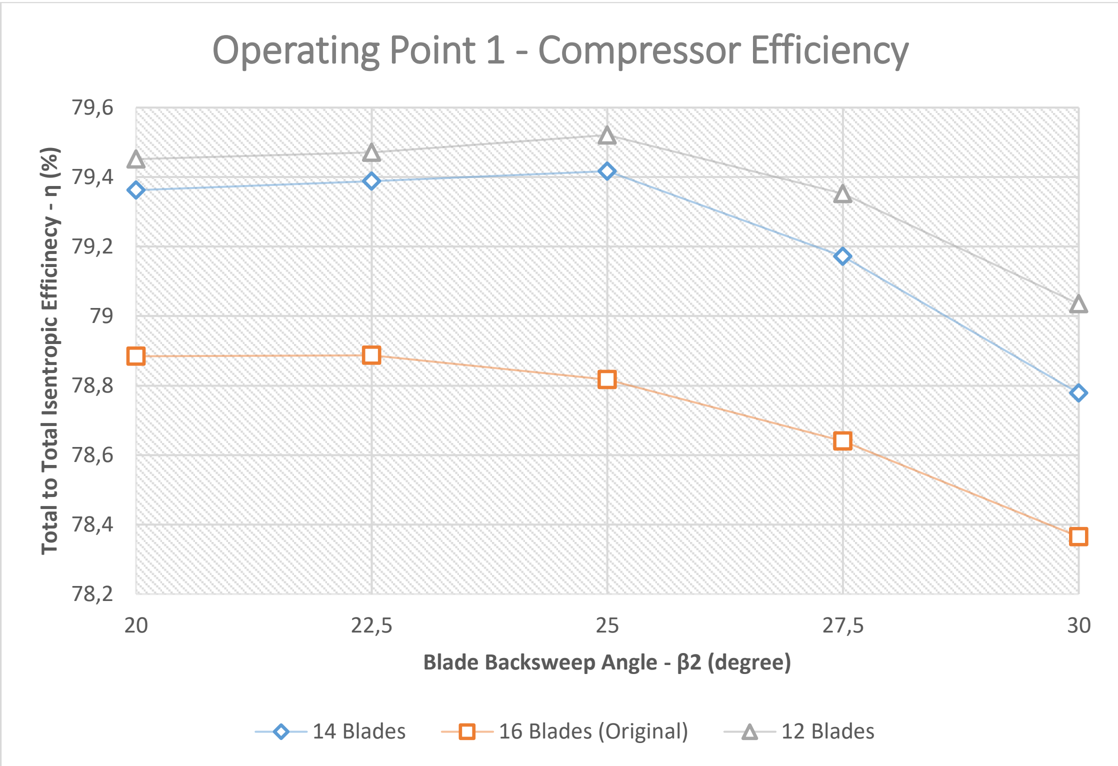

Figure 5. 3 The effect of blade backsweep angle and total number of blades on efficiency at operating point 1 (OP1)

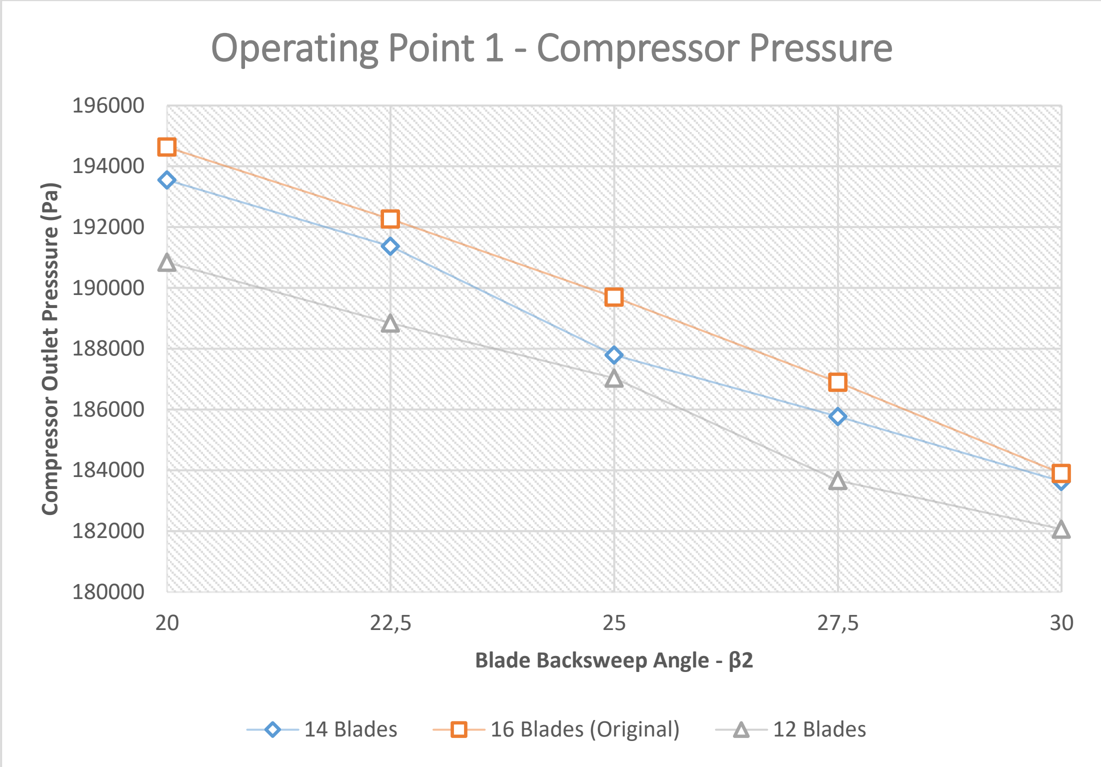

Figure 5. 4 The effect of blade backsweep angle and total number of blades on outlet pressure at operating point 1 (OP1)

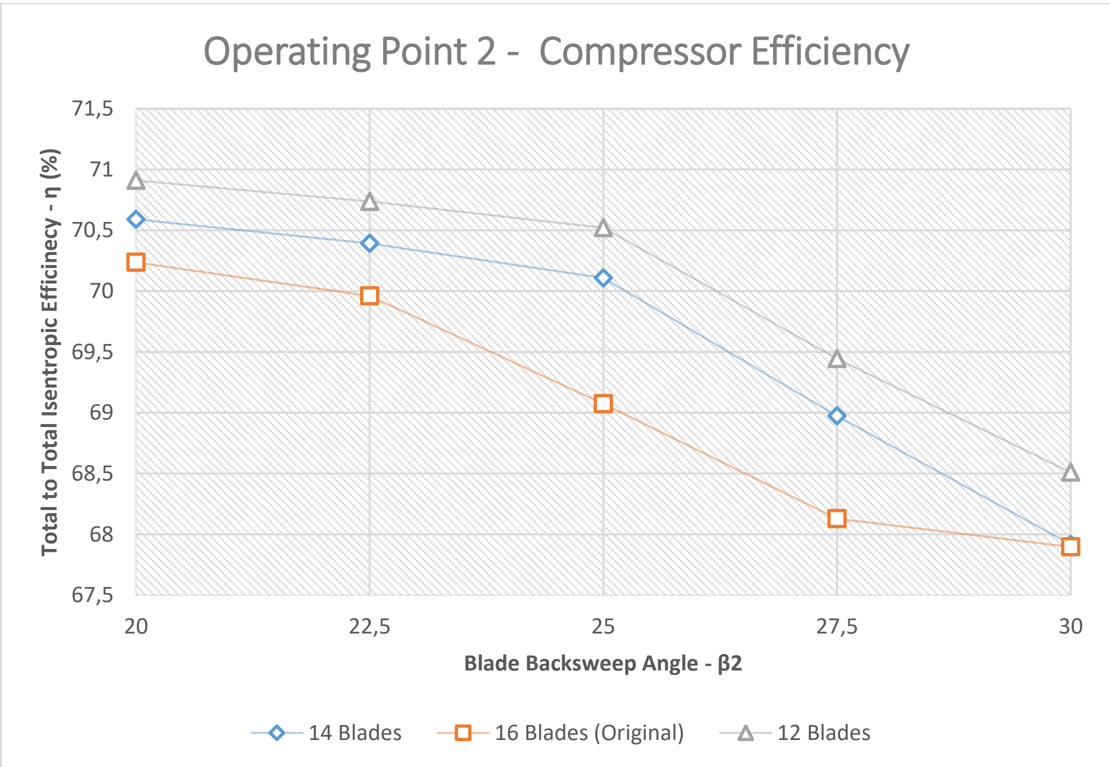

Figure 5. 5 The effect of blade backsweep angle and total number of blades on efficiency at operating point 2 (OP2)

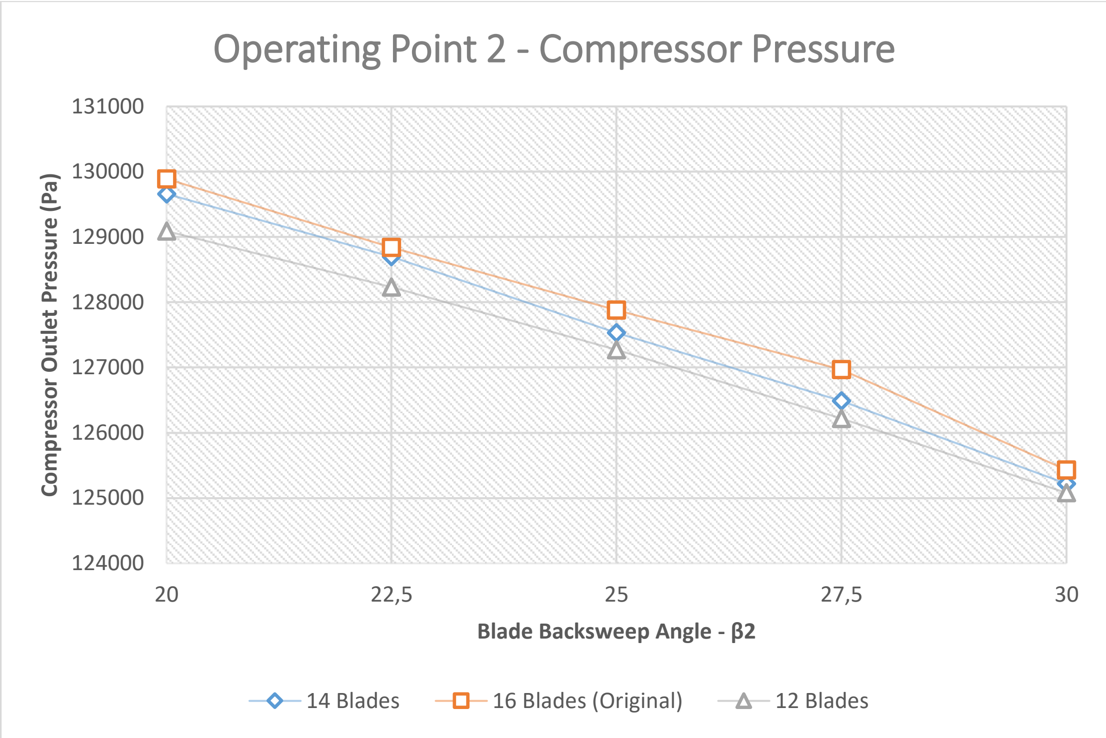

Figure 5. 6 The effect of blade backsweep angle and total number of blades on outlet pressure at operating point 2 (OP2)

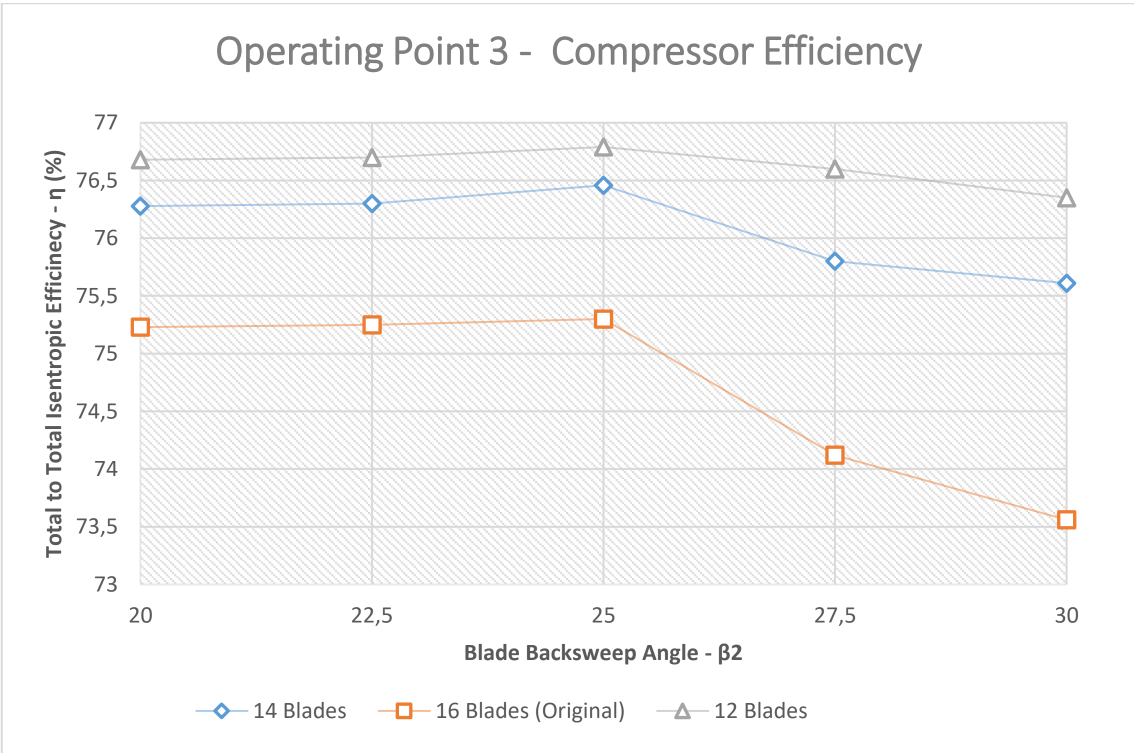

Figure 5. 7 The effect of blade backsweep angle and total number of blades on outlet pressure at operating point 3 (OP3)

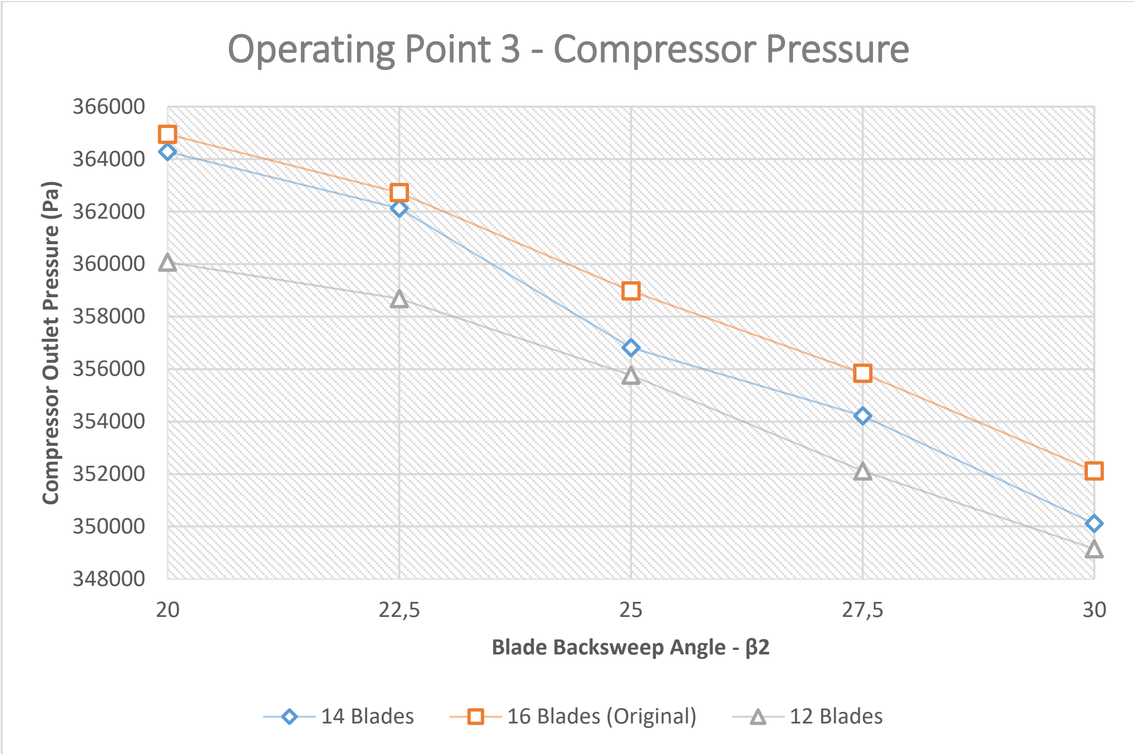

Figure 5. 8 The effect of blade backsweep angle and total number of blades on outlet pressure at operating point 3 (OP3)

5.2 New Compressor Wheel Design

The parameters, which are total number of blades and blade backsweep angle, affecting the impeller design in the existing compressor were evaluated, and a new impeller design was obtained in line with the results.

The aim of this study is to increase efficiency without changing the conditions of selected operating point. For this reason, the design with as little pressure changes as possible and high efficiency compared to the original impeller was taken as a new design. When the graphics are examined, the impeller design with total number of 14 blades and 25° backsweep angle was preferred suitable for the new design. It can be said that the design changes made by looking at the percentage changes between first, second and third operating points bring the third operating point to an optimum point. However, significant increases in compressor efficiency such as 0.77% and 1.98% were obtained at the other two operating points.

Figure 5. 9 New impeller design

5.3 New and Existing Impeller Design Result Comparison

The results of the three-dimensional CFD analyzes performed at three different operating points of the new impeller design and the existing impeller design are given in Figures 5.9, 5.10, 5.11, 5.12, 5.13, 5.14. The first three figures show the Mach number change, respectively, while the other three show the temperature change. Then the analysis results are examined, it is seen that the percentage changes of the compressor outlet pressure between the new and existing impeller designs are quite small for all three operating points, please see details in section 5.1. This means that analyzes with new and existing impeller designs run on the same points on compressor map. The Mach numbers and total temperatures in meridional view of the existing impeller design and new impeller design are shown in below figures for all three operating points.

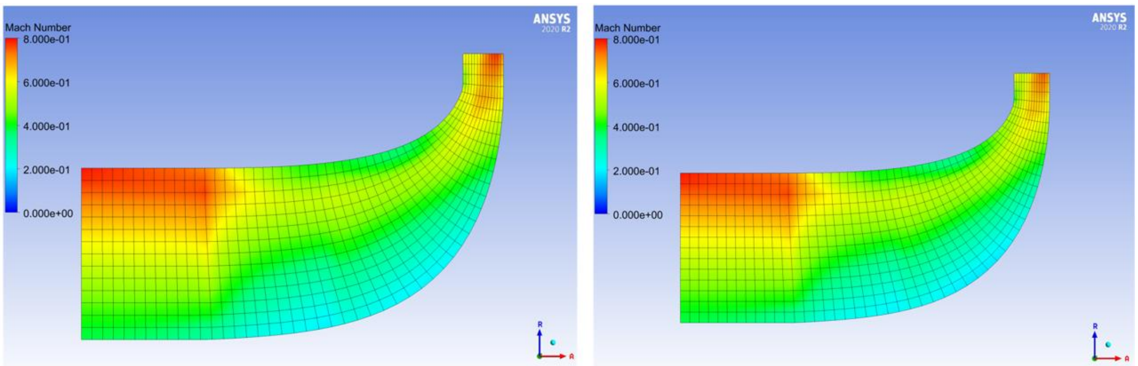

Figure 5. 10 Comparison of Mach numbers in meridional section of existing and new designs for the first operating point (OP1)

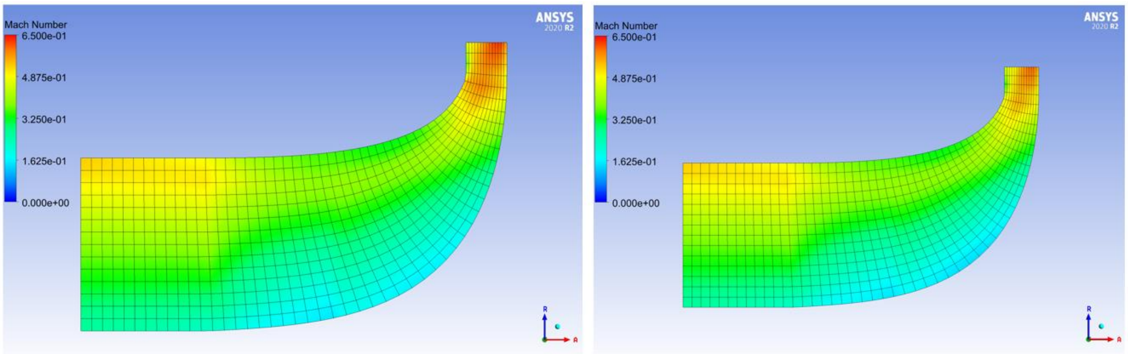

Figure 5. 11 Comparison of Mach numbers in meridional section of existing and new designs for the second operating point (OP2)

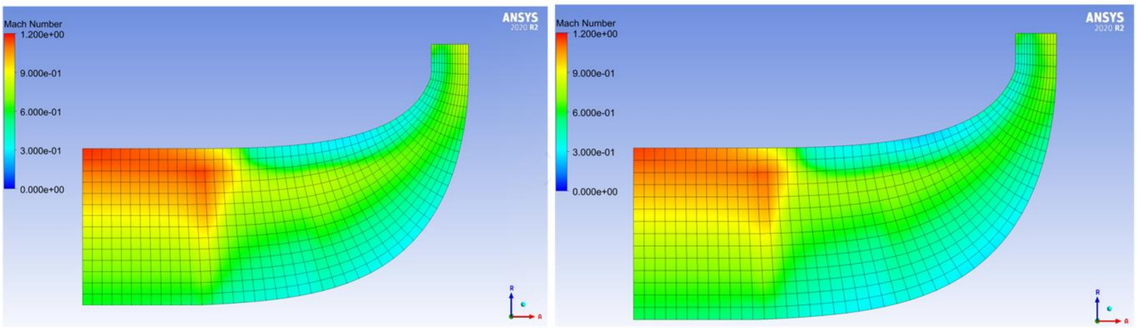

Figure 5. 12 Comparison of Mach numbers in meridional section of existing and new designs for the third operating point (OP3)

In the new impeller design, the relative Mach number is decreased, and a more homogeneous distribution has been achieved with the reduction of the swirls at the blade tip. With the blade backsweep angle changed in the new impeller design, the eddies in this region reduced, the speed is recovered, and the efficiency is increased.

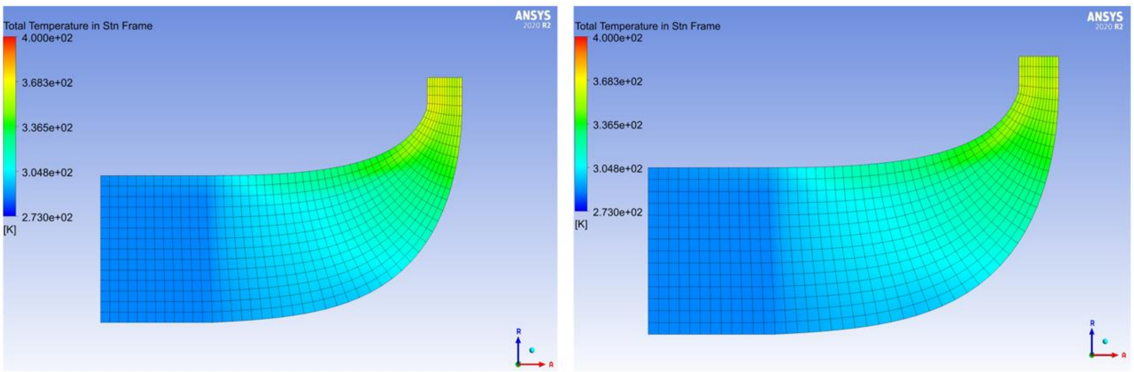

Figure 5. 13 Comparison of temperatures in meridional section of existing and new designs for the first operating point (OP1)

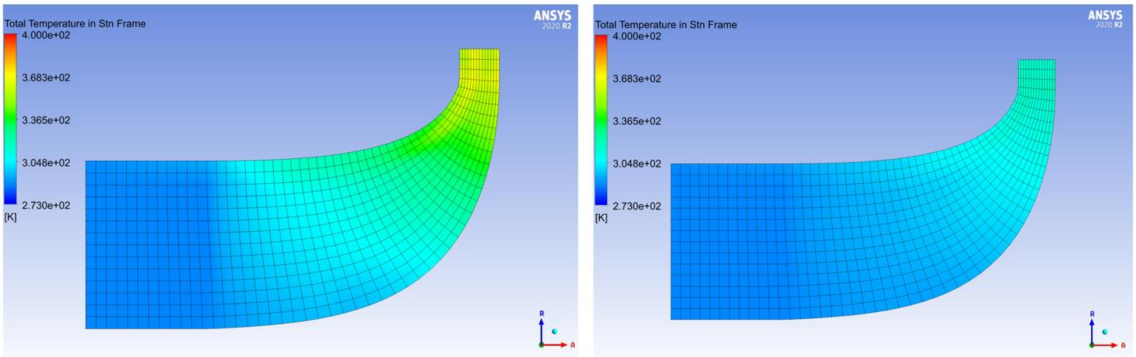

Figure 5. 14 Comparison of temperatures in meridional section of existing and new designs for the second operating point (OP2)

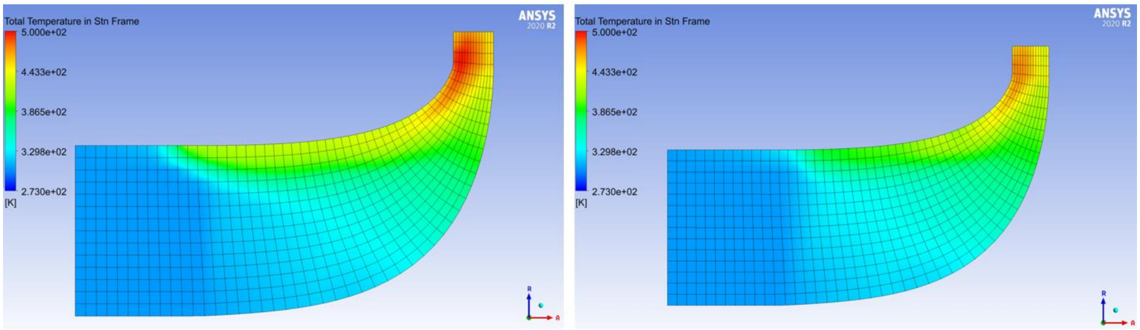

Figure 5. 15 Comparison of temperatures in meridional section of existing and new designs for the third operating point (OP3)

And there was a decrease in temperature at the compressor outlet with the increase in efficiency for all three operation points. As can be seen from the figures above, the temperature levels at the trailing edge (outlet) of the impeller were decreased.

In the study, with new impeller design, an isentropic efficiency increase is observed with a maximum of 2.34% and a minimum of 0.38% at three different operating points. However, it is seen that the effects of the total number of blades and blade outlet backsweep angle on the compressor efficiency are quite important.

REFERENCES

[1] C. Rodgers, & L. Sapiro, Design Considerations for High-Pressure-Ratio Centrifugal Compressors, ASME International Gas Turbine and Fluids Engineering Conference and Products Show, San Francisco, California, USA: March 26-30, 1972

[2] C. Rodgers, Effects of Blade Number on the Efficiency of Centrifugal Compressor Impellers, Proceedings of the ASME Turbo Expo, 2000 Rohlik, H. Analytical determination of radial inflow turbine design geometry for maximum efficiency. In National Aeronautics and Space Administration; NASA Lewis Research Center: Cleveland, OH, USA, 1969; p.4384.

[3] A. Hildebrandt, M. Genrup, 2007. Numerical Investigation of the Effect of Different Back Sweep Angle and Exducer Width on the Impeller Outlet Flow Pattern of a Centrifugal Compressor with Vaneless Diffuser, Journal of Turbomachinery 129(2): 431-433.

[4] H. Saravanamuttoo, H. Cohen, Gas Turbine Theory, 5th Edition, Pearson, 1996.

[5] R. Lewis, Turbomachinery Performance Analysis, Elsevier Science & Technology, 1996.

[6] S. Ibaraki, I. Tomita, Aerodynamic Design Optimization of Centrifugal Compressor Impeller Based on Genetic Algorithm and Artifivial Neural Network, Mitsubishi Heavy Industries Technical Review Vol. 52 No.1, March 2015.

[7] T. Wang, C. Peng, J. Wu, Back Swept ANGLE Performance Analysis of Centrifugal Compressor, ISSN 1392-1207, MECHANIKA, 2014 Volume 20(4): 302-406

[8] BorgWarner TurboSystem, turbos.borgwarner.com

[9] D. Japikse, Concepts ETI, Inc. Centrifugal Compressor Design and Performance, 1996

[10] Jeff's Diesel Repair, URL: https://jeffsdieselrepair.com/history-of-turbocharging (Access time: 09.02.2021)

[11] G. Öz, Ağır Ticari Motor İçin Turboşarj Seçimi ve Egzoz Manifoldu Tasarımı ve İmalatı (Master Thesis), Istanbul Technical University, Faculty of Engineering, Istanbul.

[12] S. Bennett, Modern Diesel Technology, Diesel Engines, Cengage Learning, 2009.

[13] J. Halderman, Automotive Engines Theory and Servicing, Eighth Edition, PEARSON, 2005

[14] G. Capon, Turbocharging the Automotive Diesel Engine, London, 2004

[15] Quora, URL: https://mrengine.quora.com/TURBOCHARGER-Turbocharger-is-a-centrifugal-compressor-powered-by-a-turbine-that-is-driven-by-exhaust-gasses-of-engine (Access time: 07.12.2021)

[16] B. Semlitsch, K.V Jyothish, Mihaescu M., Fuchs L., et al., Numerical Flow Analysis of a Centrifugal Compressor with Ported and without Ported Shroud, SAE Technical Paper, 2014-01-1655, 2014.

[17] S. Dixon, & C. Hall, Fluid Mechanics and Thermodynamics of Turbomachinery, 1998

[18] R. H. Aungier, Centrifugal Compressors, A Strategy for Aerodynamic Design and Analysis, New York, ASME Press, 2000

[19] M. A Boles, & Çengel, Y. A., 2015. Thermodynamics: An Engineering Approach. 8th ed. New York: McGraw-Hill Education

[20] CFturbo User's Guide, Turbomachinery Design, CFturbo, 2019

[21] A. Karlsson, Aerodynamic Design of Centrifugal Compressor for Heavy Duty Truck Applications. (Master Thesis), Lund University, Faculty of Engineering, Lund.

[22] Cummins Turbocharger Application Guidelines, Cumminstag.co.uk, 18.07.2021.

[23] F. Tosto, Investigation of performance and surge behavior of centrifugal compressors through CFD simulations, Master's Thesis in Fluid Dynamic, KTH Mechanics, March 2018.

[24] ANSYS CFX User's Manual, Rotating Machinery, Turbo Tools 19.1, 19.2, ANSYS 2019.

[25] S. Kim, J. Park and J. Baek, A Numerical Study of The Effects of Blade Angle Distribution on the Performance and Loss Generation of Centrifugal Compressor Impellers, Proceedings of the Institution of Mechanical Engineers, Part A: Journal of Power and Energy 2021 226:208 originally, 15 December 2011.

[26] E. Sundström, B. Kerres, M. Mihaescu, Evaluation of Centrifugal Compressor Performance Models using Large Eddy Simulation Data, Competence Center for Gas Exchange (CCGEx), KTH Machine Design, ASME Technical paper, GT2016-57169, 2016.

[27] A. Whitfield, & N. C. Baines, Design of radial turbomachines. Longman Scientific & Technical, 1990.

[28] P. M. Came and C. J. Robinson, Centrifugal Compressor Design, Proceedings of the Institution of Mechanical Engineers, Part C: Journal of Mechanical Engineering Science, 1999.

[29] W. Pulkrabek, Engineering Fundamentals of The Internal Combustion Engine, University of Wisconsin, Platteville, Prentice Hall, Upper Saddle River, New Jersey 07458.

[30] M. Norton and B. Horner, Turbocharger Fundamentals, Honeywell, 2010.

[31] Afanauto, URL: http://afanauto.com/afan-turbocharger-FAQ.html (Access time: 06.10.2021)

PUBLICATIONS FROM THE THESIS

Conference Papers

1. M. GUNEES, N. JAVANI, Performance Enhancement of Turbocharger Centrifugal Compressor, ICAME 2021 6^{th} International Conference on Advances in Mechanical Engineering, October 2021.